Identification of Novel MR1 Ligands Derived from Herbal Medicines by MR1-Presentation Reporter Screening and Their Structure-Activity Relationship

Takuro Matsuoka,[a] Akira Hattori,[a] Shinya Oishi,[a] Norihito Arichi,[a] Hideaki Kakeya,[a] Sho Yamasaki,[b, c] Hiroaki Ohno,*[a] Shinsuke Inuki*[a]

[a] Graduate School of Pharmaceutical Sciences, Kyoto University, Sakyo-ku, Kyoto 606-8501 (Japan)

E-mail: sinuki@pharm.kyoto-u.ac.jp, hohno@pharm.kyoto-u.ac.jp

[b] Research Institute for Microbial Diseases, Osaka University, Suita 565-0871 (Japan)

[c] Immunology Frontier Research Center (IFReC), Osaka University, Suita 565-0871 (Japan).

Abstract

Mucosal-associated invariant T (MAIT) cells are innate-like T cells that are modulated by ligands presented on MHC class I-related proteins (MR1). These cells have attracted attention as potential drug targets because of their involvement in the initial response to infection and various disorders. Herein, we have established the MR1-presentation reporter assay system employing split-luciferase, which enables the efficient exploration of MR1 ligands. Using our screening system, we identified herbal medicine-derived MR1 ligands, including coniferyl aldehyde, which have an ability to inhibit the MR1–MAIT cell axis. Coniferyl aldehyde comprises phenylpropanoids and is a novel motif for MR1 ligands. Further structure-activity relationship study revealed the key structural features of ligands required for MR1 recognition. These results will contribute to uncovering the mode of action of herbal medicines and their analogs, and to developing novel MAIT cell modulators.

Introduction

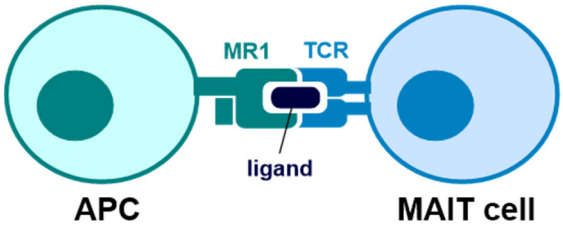

Figure 1. MR1-ligand complex recognized by T cell receptor (TCR) on MAIT cells.

Mucosal-associated invariant T (MAIT) cells are MR1-restricted T cells that are abundant in humans,[1–4] mainly in the gut, liver (45% of all α/β T cells), and peripheral blood (10% of all α/β T cells).[5] These cells are activated in response to antigens presented by MR1 on antigen-presenting cells (APC) (Figure 1). The activated MAIT cells

secrete various cytokines such as interferon-γ or interleukin-17, and/or upregulate the surface expression of CD40L molecules. These result in the activation of NK cells and conventional T cells, and the maturation of dendritic cells. Thus, MAIT cells have an important role in the initial response to infection via the amplification of immune responses.[3,6–8] MAIT cells are also involved in various diseases such as cancer and autoimmune diseases.[9–11] Therefore, MR1 ligands (antigens binding to MR1) that modulate MAIT cells are candidate vaccine adjuvants or pharmaceuticals for various disorders, including cancer and autoimmune diseases. Indeed, Pankhurst *et al*. reported that 5-(2-oxopropylideneamino)-6-D-ribitylaminouracil (5-OP-RU, a MAIT cell activator, *vide infra*) was effective as a vaccine adjuvant via the activation of dendritic cells to promote T follicular helper cell differentiation and humoral immunity.[12] In contrast, Murayama *et al*. demonstrated that the inhibition of MAIT cell activation by treatment with isobutyryl 6-formylpterin (i6-FP, *vide infra*) had beneficial effects on the disease course of lupus.[13]

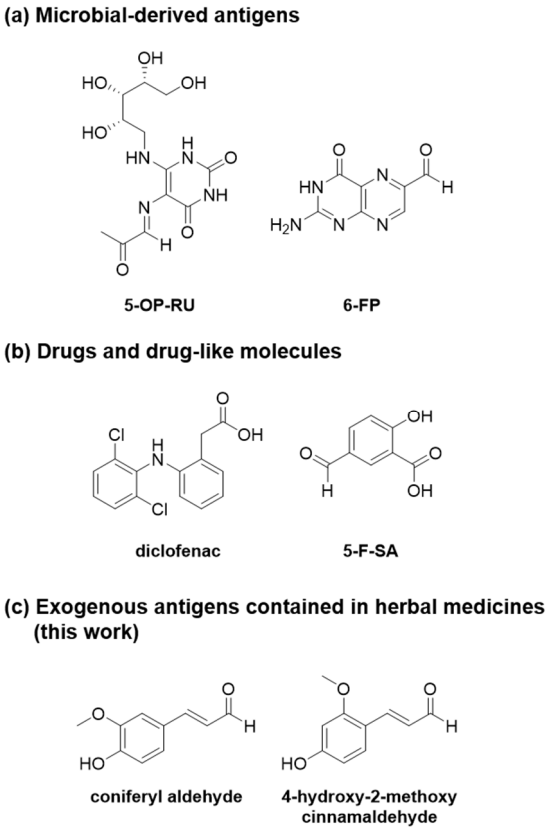

Figure 2. Representative MR1 ligands and exogenous antigens contained in herbal medicines.

MR1 ligands identified previously are mainly aromatic compounds present in microbial metabolites,[14–16] or drugs and drug-like molecules (Figures 2a and 2b).[17] As for the aromatic compounds from microbial metabolites, 5-OP-RU or 6-formylpterin (6-FP) have been identified. 5-OP-RU, a vitamin B2 metabolite, binds to MR1 and acts as a MAIT cell activator.[16] In contrast, 6-FP, a vitamin B9 metabolite, is an MR1 binder and competes with MAIT cell activators, leading to inhibition of the MR1–MAIT cell axis.[12] Additionally, several synthetic 6-FP derivatives were reported, such as acetyl 6-formylpterin (Ac-6-FP) and i6-FP (Figure S1). Regarding drugs and drug-like molecules, Keller *et al.* identified diclofenac and 5-formylsalicylic acid (5-F-SA) as an activator and an inhibitor, respectively, suggesting that the side effects and hypersensitivity caused by these drugs may be associated with the regulation of MAIT cell functions. Furthermore, Salio *et al.* reported a unique pyrimidine-based MR1 ligand that binds to MR1

and retains MR1 in the endoplasmic reticulum (ER).[18] These findings clearly indicate that the ligand-binding cleft of MR1 might be suitable for capturing structurally diverse small aromatic compounds. In addition to these reported ligands,[14–20] other endogenous and exogenous molecules might be recognized by MR1, and their identification has attracted great interest to aid our understanding of MAIT cell functions involved in various biological processes.

Here, we constructed a cell-based screening system for MR1 ligands that promote the cell-surface translocation of MR1 and regulate MAIT cell functions. Using our screening system, we found herbal medicine-derived MR1 ligands, including coniferyl aldehyde, which functioned as an inhibitor against the MR1–MAIT cell axis (Figure 2c). Further structure–activity relationship (SAR) studies revealed the key structures required for interaction with MR1.

Results and Discussion

Establishment of the MR1-presentation reporter assay employing HiBiT-LgBiT system

The antigen (ligand) presentation pathway of MR1 has been studied from functional and structural perspectives.[21–23] In the absence of ligands, MR1 exists as an apo form in the ER. With a few exceptions, MR1 typically changes conformation and migrates to the cell surface upon ligand capture, leading to the accumulation of the MR1-ligand complex on the cell surface. For example, when MR1-expressing cells are exposed to MR1 binders, 6-FP, or Ac-6-FP, the cell surface levels of MR1 were markedly increased.[24] Focusing on this presentation pathway, we constructed an MR1 ligand screening method based on the detection of the cell surface levels of MR1 as an indicator (Figure 3a), in which the HiBiT-LgBiT (split-luciferase) system was used to detect the cell surface levels of MR1. HiBiT is a small fragment of NanoLuc luciferase that binds to its complementary partner, LgBiT (non-cell permeable reporter), resulting in the emission of bright light in the presence of furimazine substrate.[25] When using cells expressing MR1 tagged by HiBiT in the extracellular domain (Figure S1a), the levels of cell-surface MR1 can be detected as luminescence intensity, allowing the identification of MR1 binders. This screening system is expected to provide a rapid and simple evaluation of the complex formation of MR1 with ligands in the cellular milieu for a vast number of compounds.

Initially, HEK293 cells stably expressing HiBiT-tagged human MR1 (HEK293.HiBiT-hMR1) were established (Figures S2a and S2b) and their functions were evaluated. When the cells were treated with known MR1 translocation-inducers (MR1 ligands), *i.e.,* Ac-6-FP, 5-F-SA and 5-OP-RU, each ligand increased the luminescence intensity (Figure 3b). These results clearly indicated that this evaluation system could detect an increase in the cell surface levels of MR1 by measuring the increase in luminescence intensity. Next, we verified that introduction of the HiBiT-tag did not affect the function of MR1. Employing flow cytometry analysis with anti-human MR1 antibody, we investigated the cell surface levels of HiBiT-tagged hMR1 in the presence of MR1 ligands, and found that all ligands tested stimulated the cell-surface translocation of both endogenous and HiBiT-tagged exogenous MR1 in a similar fashion to the increase in the reporter activity (Ac-6-FP >> 5-F-SA, 5-OP-RU, Figure S2c). Subsequently, to confirm whether complexes of HiBiT-hMR1 and a ligand were able to activate MAIT cells, we conducted a co-culture assay with HEK293.HiBiT-hMR1 cells and TG40 cells transfected with MAIT-TCR (α-chain: TRAV1-2-TRAJ33, β-chain: TRBV6-1) (TG40.MAIT-TCR) in the presence of Ac-6-FP and 5-OP-RU. We found that 5-OP-RU bound to endogenous MR1 and HiBit-hMR1 markedly activated TG40.MAIT-TCR cells, whereas Ac-6-FP did not show any activity in both cells (Figure S2d). Therefore, HiBiT-tagged MR1 binds to the ligands without impairing the original function of MR1, which can still be recognized by the MAIT-TCR,

demonstrating that HEK293.HiBiT-hMR1 cells can be useful for MR1 ligand screening. Next, the screening conditions were examined. First, we investigated how the incubation time affected the cell surface levels of MR1 and Z'-factor, a parameter used to evaluate the dynamic range of the screening system. The luminescence intensity was maximal at 4 h in the presence of Ac-6-FP and then decreased gradually (Figure S3a). The Z'-factor was highest at 8 h (Figure S3a), and this timepoint was set as the optimal incubation time. Next, the applicability of this system to a 384-well plate was investigated by collecting the activity values of a negative control (with DMSO) and a positive control (with Ac-6-FP) on the 384-well plate and calculating the Z'-factor. The Z'-factor was 0.748, indicating the tolerance of this screening system to a 384-well plate (Figure S3b).

Using these optimized conditions, we screened a commercially available compound library (LOPAC1280) consisting of 1280 biologically-active compounds (Figure S4). However, no significant increase in luminescence intensity was observed for any of the compounds. According to previous reports, most of MR1 ligands (5-OP-RU, 6-FP, Ac-6-FP, or 5-F-SA) contain carbonyl groups such as acetyl or formyl groups that can covalently anchor the ligands to MR1 via Schiff base formation with Lys43 of MR1.[14–17,24,26] Therefore, we selected 495 compounds containing carbonyl groups that might form Schiff base, from an in-house low-molecular-weight aromatic compound library. Through the screening of these compounds, we identified seven hit compounds as potent MR1 ligands (Figures 3c and 3d).

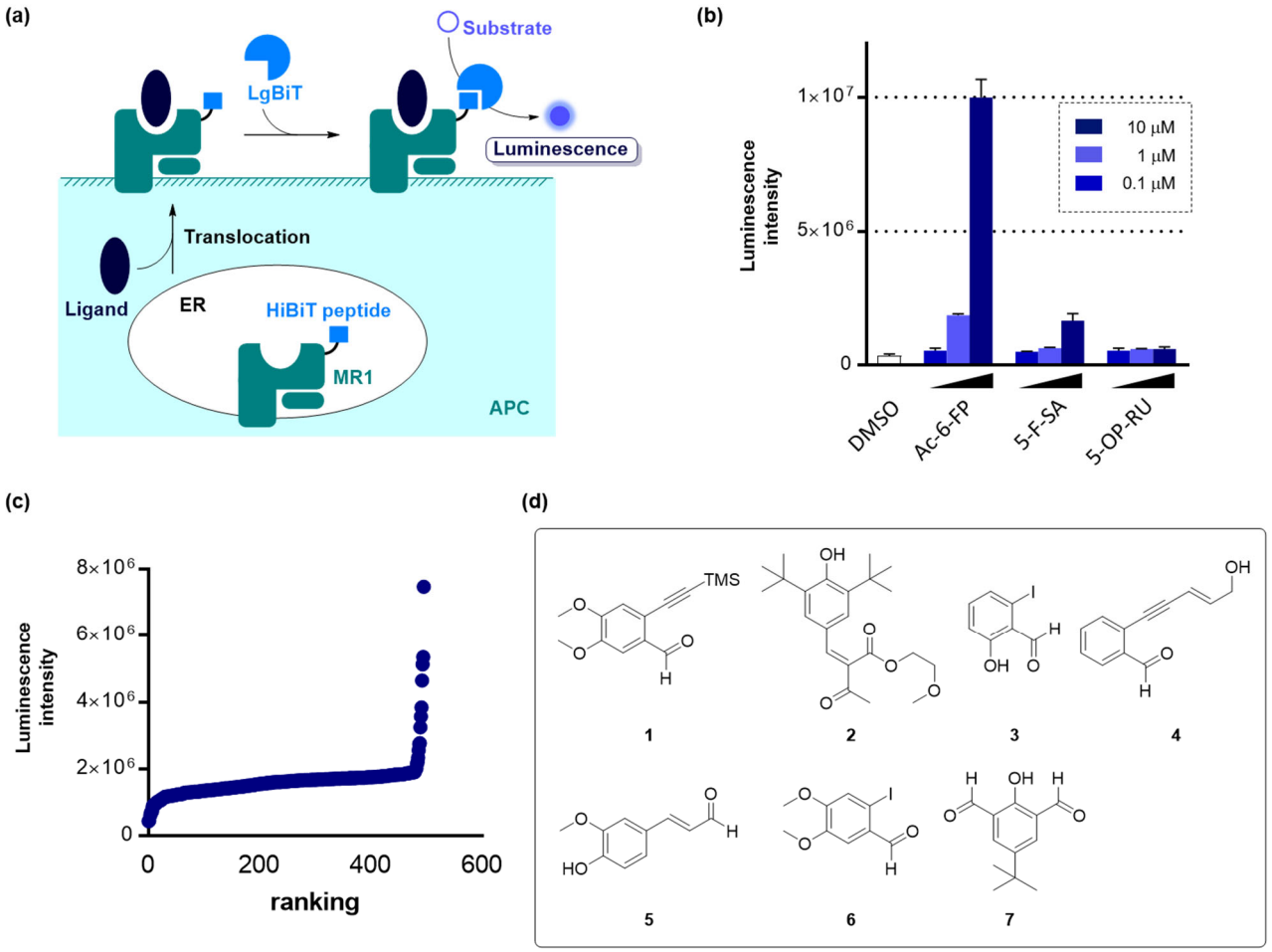

Figure 3. Establishment of the screening system. (a) Outline of the screening system. (b) Confirmation of the response of HEK293.HiBiT-hMR1 cells to known MR1 ligands. Luminescence intensity derived from cell-surface MR1 on HEK293.HiBiT-hMR1 cells was detected after 8 h incubation at 37°C in the presence of Ac-6-FP, 5-F-SA

and 5-OP-RU, followed by the addition of LgBiT and furimazine. The graphs show the mean ± SD of triplicate measurements, and the results shown are representative of three independent experiments. (c) Screening results using compounds with a carbonyl group. The cell surface levels of MR1 on HEK293.HiBiT-hMR1 cells were detected as luminescence intensity after 8 h incubation at 37°C in the presence of each compound (10 μM), followed by the addition of LgBiT and furimazine. (d) Structures of hit compounds obtained from the screening of an in-house compound library.

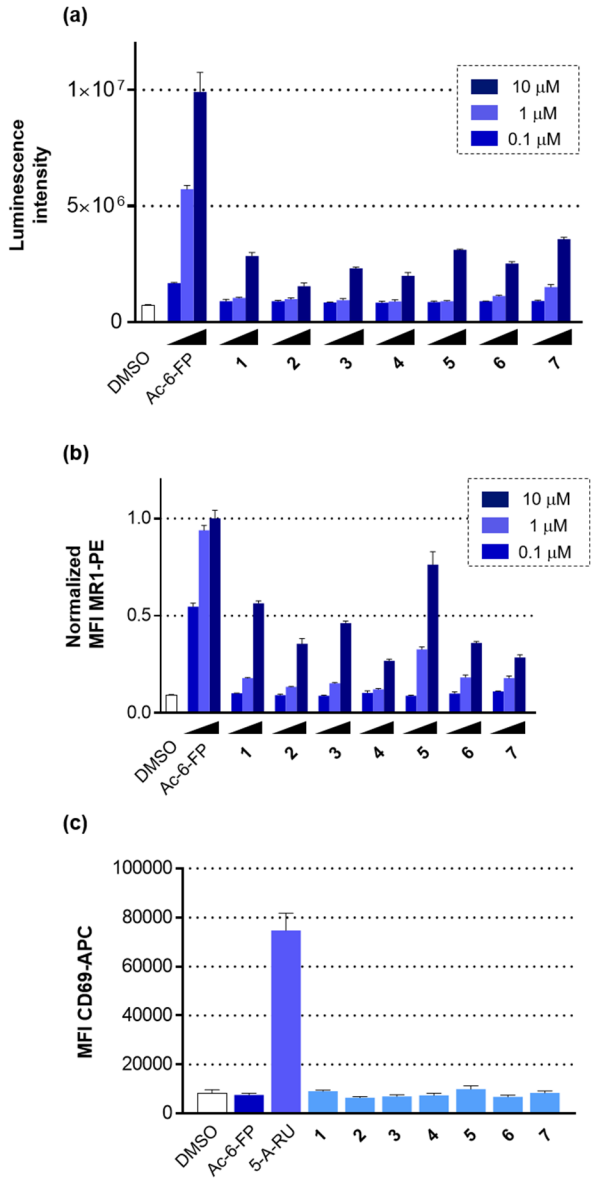

Figure 4. Validation of hit compounds. (a) Confirmation of the dose-dependency. The cell surface levels of MR1 on HEK293.HiBiT-hMR1 cells was detected as luminescence intensity after 8 h incubation at 37°C in the presence of **1**–**7**, followed by the addition of LgBiT and furimazine. (b) Flow cytometry analysis of cell-surface MR1 using HeLa.hMR1 cells expressing HiBiT-untagged hMR1. The cell surface levels of MR1 on HeLa.hMR1 cells were analyzed by flow cytometry after 8 h incubation at 37°C in the presence of **1**–**7**, followed by labeling with a PE-conjugated anti-hMR1 antibody. (c) Investigation of the ability to activate MAIT cells. Upregulation of cell surface levels of CD69, a T cell activation marker, on TG40.MAIT-TCR cells was analyzed by flow cytometry after 24 h incubation at 37°C in co-culture with HeLa.hMR1 cells in the presence of **1**–**7** (10 μM), followed by labeling with

an APC-conjugated anti-CD69 antibody. The graphs show the mean ± SD of triplicate measurements.

Validation of hit compounds

We then performed assays on the seven hit compounds (**1**–**7**) for hit validation and evaluation of their functions. As shown in Figure 4a, in compounds **1**–**7,** a dose-dependent increase in luminescence intensity attributed to the accumulation of the cell-surface MR1 level was clearly observed. The ability of each compound to increase the cell surface level of MR1 was then examined by flow cytometry analysis in human MR1-overexpressed HeLa cells (HeLa.hMR1) (Figure 4b). All the compounds stimulated the cell-surface translocation of MR1 in a dose-dependent manner, with coniferyl aldehyde (**5**) being most potent. Finally, we investigated whether TG40.MAIT-TCR cells were activated in co-culture with HeLa.hMR1 cells in the presence of each ligand. As shown in Figure 4c, none of the compounds activated TG40.MAIT-TCR cells, as in the case of Ac-6-FP. This result is consistent with previous studies reporting that the presence of a ribityl group, contained in 5-OP-RU, is essential for MAIT cell activation.[27,28]

Evaluation of natural and synthetic coniferyl aldehyde analogs

Among the hit compounds obtained in our screening, we focused on coniferyl aldehyde (**5**), a potent upregulator of cell surface MR1 levels. Coniferyl aldehyde (**5**) is an exogenous antigen found in herbal medicines with anti-inflammatory properties, such as *Cinnamomum cassia,* or dietary ingredients such as black sesame.[29–31] These findings suggest that the regulatory effect of coniferyl aldehyde (**5**) on MAIT cell activation may be, at least partially, related to the mode of action of these herbal medicines or dietary ingredients.

Coniferyl aldehyde (**5**) is a phenylpropanoid, and its analogs are found in herbal medicines and edible plants (Figure 5a). Thus, we speculated that a comprehensive evaluation of these compounds would provide new insights into the relationship between herbal medicines or edible plants and MAIT cells. The natural analogs derived from herbal medicines and edible plants were synthesized, and their ability to increase the cell surface level of MR1 was evaluated by flow cytometry analysis using HeLa.hMR1 cells (Figures 5b, S5a and S5b). Analogs with no or one electron-donating substituent on a benzene ring had no activity (**8**–**15**). Conversely, analogs **16** and **17** strongly increased the cell surface levels of MR1. Analog **16** is derived from *Andrographis paniculata*, a medicinal plant used mainly in Southeast Asia for its efficacy in relieving inflammation and pain,[32] and analog **17** is contained in a poisonous plant, *Phytolacca americana*.[33] The reciprocal exchange of a substituent on the benzene ring (**18**) and introduction of a prenyl group at the 3-position (**19**) significantly reduced the activity. Derivatives with a dimethoxy group at the 3- and 5-positions (**20**) and dioxole (**21**, **22**) also had little activity.

In addition to natural analogs, we performed another SAR study using synthetic coniferyl aldehyde derivatives (Figures 5c and S5b). Saturated derivative **23** and two-carbon degraded/homologated derivatives (**24**, **25**) had no activity. On the basis of the reported analysis of ligand-MR1 interactions, the formyl group in coniferyl aldehyde is expected to form a Schiff base with the Lys43 of MR1, which promotes MR1 refolding and translocation to the cell surface. Actually a derivative with an acetyl group (**26**) showed a little activity, and derivatives with a carboxy group (**27**) or nitrile group (**28**) had no activity. Therefore, the formyl group in **5** is essential for its translocation to the cell surface, suggesting that this functional group might form a Schiff base with the Lys43 of MR1, similar to other MR1 ligands such as Ac-6FP or 5-F-SA. We also performed a SAR study on the benzene ring of **5**. Removing the phenolic hydroxy group (**29**) or changing the position of the phenolic hydroxy group from the 4-position to the 2-position (**30**) greatly weakened its activity. The introduction of a dimethylamino group instead of a methoxy group did not

influence the cell surface levels of MR1 (**31**). A 2,5-dimethoxy derivative (**32**) increased the cell surface levels of MR1 to a greater extent than the 3,5-dimethoxy derivative (**20**, natural analog). A pyridone analog (**33**) and bicyclic derivative (**34**) had little potency. Taken together, these SAR studies indicate that the α,β-unsaturated aldehyde structure and the phenolic hydroxy group at the 4-position are crucial for the ligand-induced cell surface translocation of MR1.

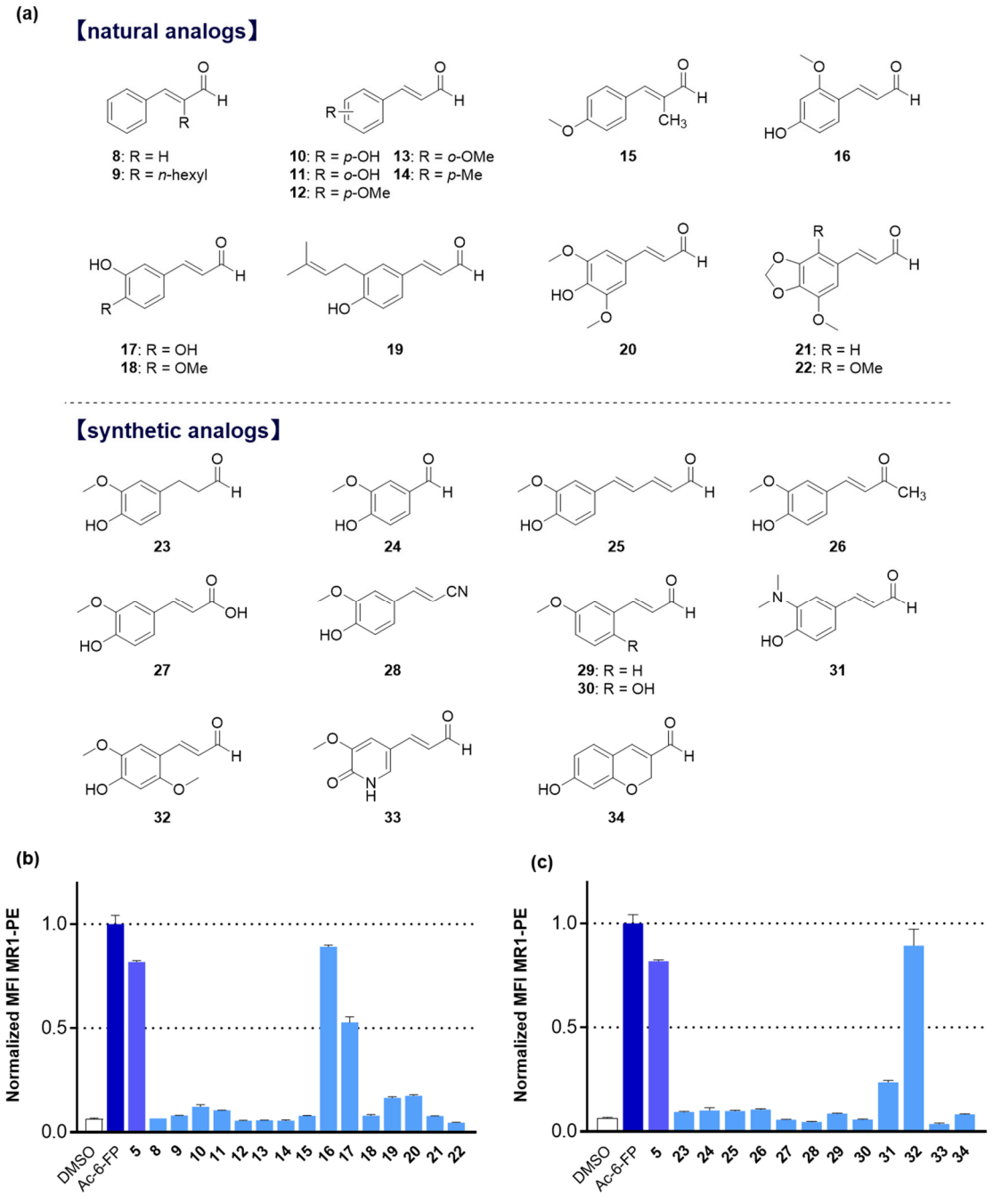

Figure 5. Evaluation of coniferyl aldehyde analogs. (a) Structures of the tested compounds. The cell surface levels of MR1 on HeLa.hMR1 cells were analyzed by flow cytometry after 8 h incubation at 37°C in the presence of (b) natural analogs (**8**–**22**) (10 μM) or (c) synthetic analogs (**23**–**34**) (10 μM), followed by labeling with a PE-conjugated anti-hMR1 antibody. The graphs show the mean ± SD of triplicate measurements, and the results shown are representative of at least three independent experiments.

Functional analysis of newly identified MR1 ligands

Next, we performed detailed analyses of the derivatives **5**, **16**, **17** and **32** identified as MR1 upregulators (Figure 6). Although an apparent dose-dependency in the cell-surface translocation of MR1 was observed for all derivatives (Figure 6a), an increase in T cell activation marker CD69 was not detected for these compounds (Figure 6b). We next examined the inhibitory activity of coniferyl aldehyde (**5**) and its analogs against the 5-OP-RU-induced MAIT cell activation. We found that all compounds, including Ac-6-FP, restrained the activation of MAIT cells by 5-OP-RU (Figure 6c). This indicated that these compounds were accommodated within the MR1 binding cleft and competed with 5-OP-RU, similar to 6-FP or Ac-6-FP. Subsequently, MR1-specific presentation of the compounds was investigated by flow cytometry analysis employing anti-human HLA-A/B/C antibody. In Figure 6d, no significant increase in the cell surface levels of HLA-A/B/C, classical human MHC class I molecules was observed in all compound-treated HeLa.hMR1 cells. These results strongly indicated that coniferyl aldehyde and its analogs are specifically presented to MR1, which promotes the cell-surface translocation of MR1 but not stimulating the global exocytosis.

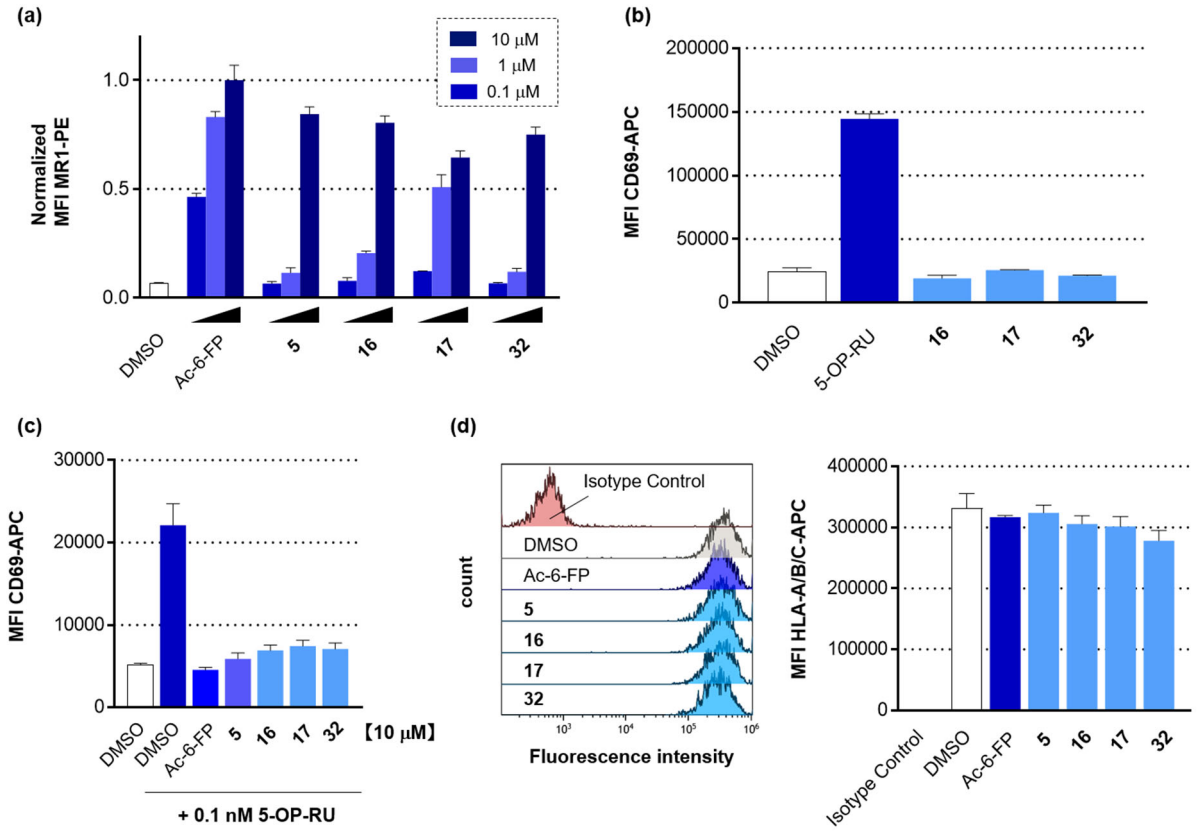

Figure 6. Functional analysis of the coniferyl aldehyde analogs. (a) Confirmation of dose-dependency. The cell surface levels of MR1 on HeLa.hMR1 cells were analyzed by flow cytometry after 8 h incubation at 37°C in the presence of coniferyl aldehyde (**5**) or its analogs, followed by labeling with a PE-conjugated anti-hMR1 antibody. (b) Investigation of the ability of analogs to activate MAIT cells. Upregulation of cell surface levels of CD69 on TG40.MAIT-TCR cells was analyzed by flow cytometry after 24 h incubation at 37°C in co-culture with HeLa.hMR1 cells in the presence of coniferyl aldehyde (**5**) or its analogs (10 μM), followed by labeling with an APC-conjugated anti-CD69 antibody. (c) Investigation of the inhibitory activity of MAIT cell activation. Upregulation of cell surface levels of CD69 on TG40.MAIT-TCR cells was analyzed by flow cytometry after 24 h

incubation at 37°C in co-culture with HeLa.hMR1 cells in the presence of coniferyl aldehyde (**5**) or its analogs (10 μM) and 5-OP-RU (0.1 nM), followed by labeling with an APC-conjugated anti-CD69 antibody. (d) Effects of coniferyl aldehyde (**5**) and its analogs on the cell surface levels of HLA-A/B/C. The cell surface levels of HLA-A/B/C on HeLa.hMR1 cells were analyzed by flow cytometry after 8 h incubation at 37°C in the presence of coniferyl aldehyde (**5**) or its analogs, followed by labeling with an APC-conjugated anti-HLA-A/B/C antibody. The graphs show the mean ± SD of triplicate measurements, and the results shown are representative of three independent experiments.

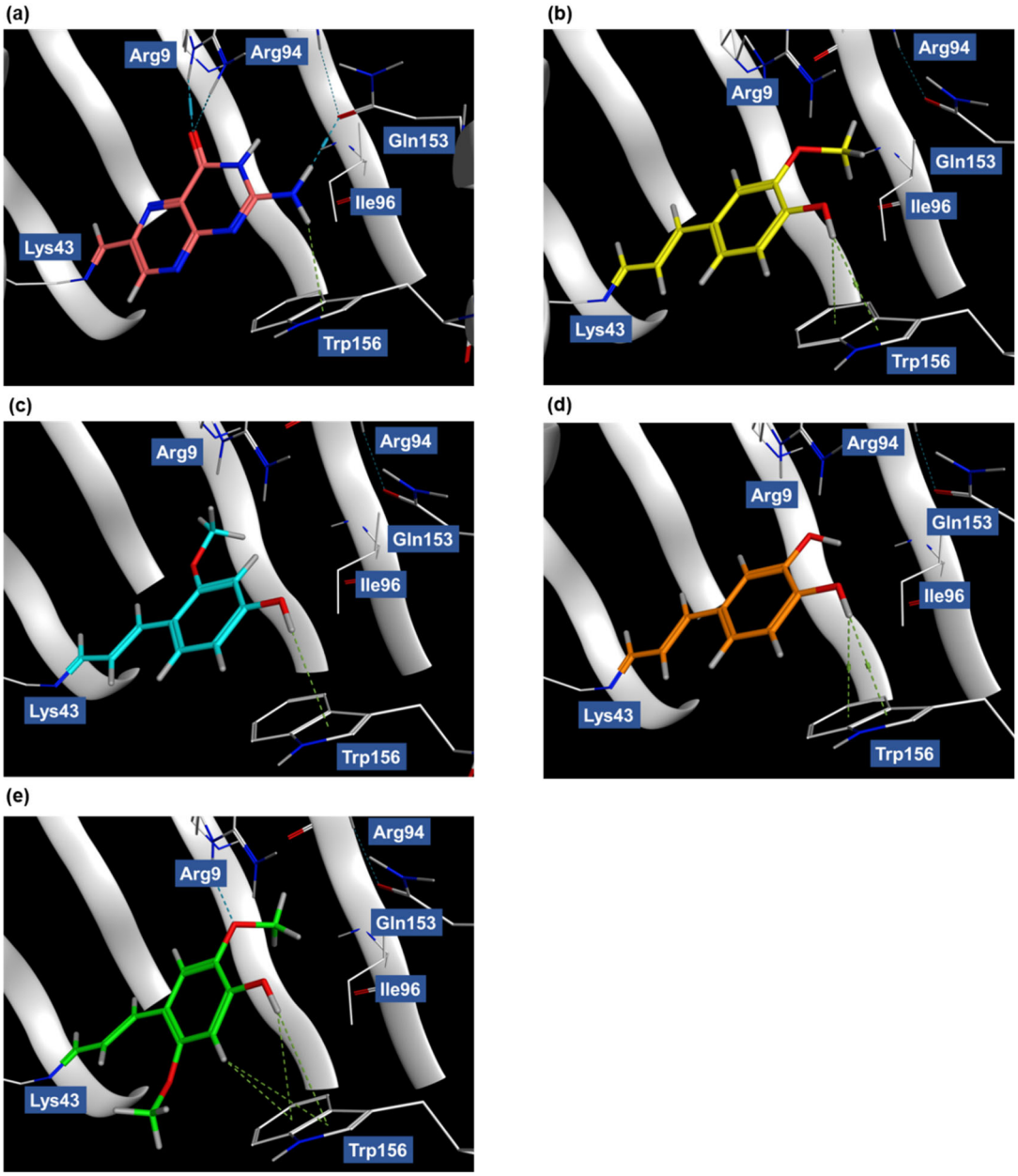

Figure 7. Binding mode analysis of (a) 6-FP, (b) **5**, (c) **16**, (d) **17** and (e) **32** with the MR1-ligand binary complex (PDB ID: 4GUP) as a template. Green dashed lines: interactions with π-electron system. Blue dashed lines: hydrogen bonds.

Binding mode analysis of coniferyl aldehyde analogs

Finally, we analyzed the binding mode of the coniferyl aldehyde (**5**) and its derivatives (**16**, **17** and **32**) to MR1 with the molecular operating environment (MOE). The reported X-ray crystal structure of MR1 with 6-FP (PDB ID: 4GUP) was used as a template for the preparation of binding models. On the basis of prior research and our SAR study of coniferyl aldehyde (**5**), we performed the analysis under the assumption that the formyl group in coniferyl aldehyde (**5**) would covalently bind to MR1 via the Schiff base with Lys43. As shown in Figure 7, the phenolic hydroxy group at the 4-position in all compounds, bound to the indole ring of Trp156 through OH-π interactions. Furthermore, hydrogen bonding between the methoxy group in **32** and a guanidine group in Arg9 was observed. These interactions were also found in the original structure of MR1 with 6-FP; an amino group interacts with Trp156 through NH-π interaction, and a carbonyl group forms a hydrogen bond to Arg9. Given the importance of the phenolic hydroxy group at the 4-position shown in the SAR study, the OH-π interaction with Trp156 might be a key factor for binding to MR1.

Conclusion

MAIT cells play pivotal roles in innate immunity and their malfunction leads to immunological disorders such as cancer and autoimmune diseases. Therefore, the identification of MAIT cell modulators (activators and inhibitors) for the development of pharmaceuticals/immune adjuvants has recently attracted significant attention.

In this study, we developed the MR1-presentation reporter assay system with split-luciferase, enabling the efficient identification of MR1 ligands. Using this system, we identified novel MR1 binders derived from herbal medicines and edible plants (coniferyl aldehyde (**5**) and its analogs), and found that they were recognized by MR1 ligand binding cleft, and inhibited MAIT cell activation induced by 5-OP-RU. Coniferyl aldehyde (**5**) and its analog (**16**) are present in dietary components such as edible plants and herbal medicines with anti-inflammatory activities. These results imply that the regulation of MAIT cell functions might be, at least partially, associated with their anti-inflammatory activities.

In terms of ligand structures, known MR1 ligands commonly include pterin, pyrimidine or benzaldehyde derivatives. Coniferyl aldehyde (**5**) and its analog (**16**) consist of phenylpropanoids, which is a novel motif for MR1 ligands. The SAR study revealed that the α,β-unsaturated aldehyde structure and the phenolic hydroxy group at the 4-position are necessary for presentation by MR1. Further binding mode analysis suggested that the OH-π interaction with Trp156 might be associated with the interaction with MR1.

The screening system newly developed in this study will contribute to the identification of a broader range of MR1 ligands, including endogenous and exogenous antigens, with implications for our understanding of MAIT cell functions. Furthermore, coniferyl aldehyde (**5**) and its analogs might be promising leads for the development of novel MAIT cell modulators, and the SAR studies could provide guidelines for ligand design.

Experimental section

Chemistry

^{1}H NMR spectra were recorded using a JEOL ECA-500 or JEOL ECZ600R spectrometer. Chemical shifts are reported in δ (ppm) relative to Me_4Si (in $CDCl_3$ or DMSO-d_6) as internal standard. ^{13}C NMR spectra were recorded using a JEOL ECA-500 or JEOL ECZ600R and referenced to the residual $CHCl_3$ signal (in $CDCl_3$) and the residual DMSO signal (in DMSO-d_6). Exact mass (HRMS) spectra were recorded on a Shimadzu LC-ESI-IT-TOF-MS equipment (ESI). IR spectra were obtained on a JASCO FT/IR-4100 spectrometer. Synthetic method for compounds **5**[34], **15**[35], **23**[36], **28**[37], **34**[38], **S1**[39], **S3**[39], **S11**[40], **S13**[41], **S18**[42], **S21**[43], **S23**[44], **S25**[45], **S27**[46], **S31**[47], **S33**[48], **S37**[49] and **S41**[50] are reported. Compounds **8**, **9**, **24**, **27**, **S5**, **S7**, **S9**, **S15** and **S29** are commercially available. Structures of **S1**–**S45** are shown in Schemes S1–S12. All tested compounds have a purity of >95% determined by HPLC (Supporting Information).

(*E*)-3-(4-Hydroxyphenyl)acrylaldehyde (10).

The mixture of **S1** (169 mg, 1.02 mmol), (1,3-dioxolan-2-yl)methyltriphenylphosphonium bromide 651 mg, 1.52 mmol), K_2CO_3 (208 mg, 1.50 mmol) and 18-crown-6 (6.38 mg, 0.0241 mmol) in toluene (10.0 mL) was stirred at 100 °C. After being stirred for 21 h at this temperature under Ar, the mixture was diluted with EtOAc. The whole was washed with H_2O and brine, and dried over $MgSO_4$. After concentration *in vacuo*, the residue was purified by flash chromatography over NH_2 silica gel with *n*-hexane–EtOAc (5:1) to give a crude **S2** (193 mg), which was used without further purification. Then, to a stirred solution of **S2** (118 mg) in THF (14.3 mL) was added aqueous solution of HCl (10%; 7.14 mL). After being stirred for 2 h at 50 °C, the mixture was diluted with saturated aqueous solution of $NaHCO_3$. The whole was extracted with EtOAc, washed with H_2O and brine, and dried over $MgSO_4$. After concentration *in vacuo*, the residue was purified by flash chromatography over silica gel with a gradient of 6% to 40% EtOAc in *n*-hexane to afford **10** (57.2 mg, 62%, 2 steps): pale yellow solid; mp 144–145 °C; IR (neat cm^{-1}): 1642 (C=O); ^{1}H NMR (500 MHz, $CDCl_3$) δ 5.69 (s, 1H), 6.62 (dd, J = 15.5, 8.0 Hz, 1H), 6.89–6.92 (m, 2H), 7.44 (d, J = 15.5 Hz, 1H), 7.47–7.51 (m, 2H), 9.65 (d, J = 8.0 Hz, 1H); ^{13}C{^{1}H} NMR (150 MHz, $CDCl_3$) δ 116.1 (2C), 126.4, 127.0, 130.7 (2C), 153.1, 158.7, 194.1; HRMS (ESI-TOF) *m/z*: $[M - H]^-$ calcd for $C_9H_7O_2$, 147.0452; found, 147.0453. The purity of **10** was >99% as determined by HPLC.

(*E*)-3-(2-Hydroxyphenyl)acrylaldehyde (11)

By a procedure identical with that described for synthesis of **S2** from **S1**, the benzaldehyde **S3** (82.9 mg, 0.499 mmol) was converted into a crude **S4** (58.7 mg), which was used without further purification. Then, by a procedure similar to that described for synthesis of **10** from **S2**, the crude acetal **S4** (46.8 mg) was converted into the aldehyde **11** (16.1 mg, 27% yield, 2 steps). Column chromatography: silica gel (gradient 6% to 30% EtOAc in *n*-hexane): pale yellow solid; mp 131–133 °C; IR (neat cm^{-1}): 3212 (OH), 1658 (C=O); ^{1}H NMR (500 MHz, $CDCl_3$) δ 5.74 (s, 1H), 6.84–6.86 (m, 1H), 6.92 (dd, J = 16.0, 8.0 Hz, 1H), 6.98–7.01 (m, 1H), 7.30–7.33 (m, 1H), 7.53 (dd, J = 7.7, 1.4 Hz, 1H), 7.80 (d, J = 16.0 Hz, 1H), 9.70 (d, J = 8.0 Hz, 1H); ^{13}C{^{1}H} NMR (150 MHz, $CDCl_3$) δ 116.5, 121.0, 121.3, 129.2, 130.2, 132.7, 149.9, 155.7, 195.9; HRMS (ESI-TOF) *m/z*: $[M + H]^+$ calcd for $C_9H_9O_2$, 149.0597; found, 149.0597. The purity of **11** was 98% as determined by HPLC.

(*E*)-3-(4-Methoxyphenyl)acrylaldehyde (12)

By a procedure identical with that described for synthesis of **S2** from **S1**, the benzaldehyde **S5** (136 mg, 1.00 mmol) was converted into a crude **S6** (89.2 mg), which was used without further purification. Then, by a procedure similar to that described for synthesis of **10** from **S2**, the crude acetal **S6** (59.8 mg) was converted into the aldehyde **12** (37.6 mg, 35% yield, 2 steps). Column chromatography: silica gel (gradient 4% to 25% EtOAc in *n*-hexane): white solid; mp 54–56 °C; IR (neat cm^{-1}): 1672 (C=O); ^1H NMR (500 MHz, $CDCl_3$) δ 3.87 (s, 3H), 6.62 (dd, J = 15.8, 7.7 Hz, 1H), 6.94–6.97 (m, 2H), 7.43 (d, J = 15.8 Hz, 1H), 7.52–7.55 (m, 2H), 9.66 (d, J = 7.7 Hz, 1H); $^{13}C\{^1H\}$ NMR (150 MHz, $CDCl_3$): δ 55.4, 114.5 (2C), 126.5, 126.7, 130.4 (2C), 152.8, 162.2, 193.8; HRMS (ESI-TOF) *m/z*: $[M + H]^+$ calcd for $C_{10}H_{11}O_2$, 163.0754; found, 163.0755. The purity of **12** was 96% as determined by HPLC.

(*E*)-3-(2-Methoxyphenyl)acrylaldehyde (13)

By a procedure identical with that described for synthesis of **S2** from **S1**, the benzaldehyde **S7** (137 mg, 1.01 mmol) was converted into a crude **S8** (227 mg), which was used without further purification. Then, by a procedure similar to that described for synthesis of **10** from **S2**, the crude acetal **S8** (42.3 mg) was converted into the aldehyde **13** (65.5 mg, 89% yield, 2 steps). Column chromatography: silica gel (gradient 6% to 26% EtOAc in *n*-hexane): colorless oil; IR (neat cm^{-1}): 1671 (C=O); ^1H NMR (500 MHz, $CDCl_3$) δ 3.92 (s, 3H), 6.80 (dd, J = 16.0, 8.0 Hz, 1H), 6.95–6.96 (m, 1H), 6.99–7.05 (m, 1H), 7.40–7.44 (m, 1H), 7.56 (dd, J = 7.4, 1.7 Hz, 1H), 7.85 (d, J = 16.0 Hz, 1H), 9.70 (d, J = 8.0 Hz, 1H); $^{13}C\{^1H\}$ NMR (150 MHz, $CDCl_3$): δ 55.5, 111.2, 120.8, 122.9, 128.8, 129.1, 132.7, 148.3, 158.2, 194.6; HRMS (ESI-TOF) *m/z*: $[M + H]^+$ calcd for $C_{10}H_{11}O_2$, 163.0754; found, 163.0752. The purity of **13** was 99% as determined by HPLC.

(*E*)-3-(*p*-Tolyl)acrylaldehyde (14)

By a procedure identical with that described for synthesis of **S2** from **S1**, the benzaldehyde **S9** (60.1 mg, 0.500 mmol) was converted into a crude **S10** (58.1 mg), which was used without further purification. Then, by a procedure similar to that described for synthesis of **10** from **S2**, the crude acetal **S10** (58.1 mg) was converted into the aldehyde **14** (35.0 mg, 39% yield, 2 steps). Column chromatography: silica gel (gradient 4% to 17% EtOAc in *n*-hexane): white amorphous; IR (neat cm^{-1}): 1682 (C=O); ^1H NMR (500 MHz, $CDCl_3$) δ 2.40 (s, 3H), 6.69 (dd, J = 16.0, 7.8 Hz, 1H), 7.24 (d, J = 8.2 Hz, 2H), 7.44–7.51 (m, 3H), 9.69 (d, J = 7.8 Hz, 1H); $^{13}C\{^1H\}$ NMR (150 MHz, $CDCl_3$): δ 21.5, 127.6, 128.4 (2C), 129.8 (2C), 131.2, 141.9, 153.0, 193.8; HRMS (ESI-TOF) *m/z*: $[M + H]^+$ calcd for $C_{10}H_{11}O$, 147.0804; found, 147.0798. The purity of **14** was 98% as determined by HPLC.

(*E*)-3-(4-Hydroxy-2-methoxyphenyl)acrylaldehyde (16)

By a procedure identical with that described for synthesis of **S2** from **S1**, the benzaldehyde **S11** (98.1 mg, 0.500 mmol) was converted into a crude **S12** (32.8 mg), which was used without further purification. Then, by a procedure similar to that described for synthesis of **10** from **S2**, the crude acetal **S12** (25.3 mg) was converted into the aldehyde **16** (15.0 mg, 22% yield, 2 steps). Column chromatography: silica gel (gradient 12% to 55% EtOAc in *n*-hexane): pale yellow solid; mp 143–144 °C; IR (neat cm^{-1}): 1658 (C=O); ^1H NMR (500 MHz, $CDCl_3$) δ 3.89 (s, 3H), 5.34 (s, 1H), 6.45–6.48 (m, 2H), 6.70 (dd, J = 15.8, 8.0 Hz, 1H), 7.45 (d, J = 8.0 Hz, 1H), 7.74 (d, J = 15.8 Hz, 1H), 9.63 (d, J = 8.0 Hz, 1H); $^{13}C\{^1H\}$ NMR (150 MHz, $CDCl_3$) δ 55.6, 99.1, 108.2, 116.0, 126.5, 130.8, 149.2, 160.3, 160.4,

195.1; HRMS (ESI-TOF) *m/z*: $[M + H]^+$ calcd for $C_{10}H_{11}O_3$, 179.0703; found, 179.0703. The purity of **16** was >99% as determined by HPLC.

(*E*)-3-(3,4-Dihydroxyphenyl)acrylaldehyde (17)

By a procedure identical with that described for synthesis of **S2** from **S1**, the benzaldehyde **S13** (228 mg, 1.01 mmol) was converted into a crude **S14** (151 mg), which was used without further purification. Then, by a procedure similar to that described for synthesis of **10** from **S2**, the crude acetal **S14** (151 mg) was converted into the aldehyde **17** (33.4 mg, 20% yield, 2 steps). Column chromatography: silica gel (gradient 12% to 80% EtOAc in *n*-hexane): white solid; mp 198–200 °C; IR (neat cm^{-1}): 1685 (C=O); ^1H NMR (500 MHz, DMSO-d_6) δ 6.53 (dd, J = 16.0, 8.0 Hz, 1H), 6.81 (d, J = 8.6 Hz, 1H), 7.06–7.10 (m, 2H), 7.55 (d, J = 16.0 Hz, 1H), 9.56 (d, J = 8.0 Hz, 1H); $^{13}C\{^1H\}$ NMR (150 MHz, DMSO-d_6) δ 115.3, 115.9, 122.1, 125.3, 125.6, 145.7, 149.3, 154.3, 194.0; HRMS (ESI-TOF) *m/z*: $[M - H]^-$ calcd for $C_9H_7O_3$, 163.0401; found, 163.0401. The purity of **17** was 99% as determined by HPLC.

4-Methoxy-3-(methoxymethoxy)benzaldehyde (S16)

To a solution of **S15** (763 mg, 5.01 mmol) and K_2CO_3 (2.81 g, 20.3 mmol) in DMF (2.94 mL) was added MOMCl (570 μL, 7.50 mmol). After being stirred for 5.5 h at room temperature under Ar, the mixture was diluted with H_2O. The whole was extracted with Et_2O, washed with H_2O and brine, and dried over $MgSO_4$. After concentration *in vacuo*, the residue was purified by flash chromatography over silica gel with a gradient of 6% to 40% EtOAc in *n*-hexane to give **S16** (887 mg, 90% yield): white amorphous; IR (neat cm^{-1}): 1687 (C=O); ^1H NMR (500 MHz, $CDCl_3$) δ 3.53 (s, 3H), 3.98 (s, 3H), 5.29 (s, 2H), 7.02 (d, J = 8.0 Hz, 1H), 7.55 (dd, J = 8.0, 1.7 Hz, 1H), 7.67 (d, J = 1.7 Hz, 1H), 9.86 (s, 1H); $^{13}C\{^1H\}$ NMR (150 MHz, $CDCl_3$) δ 56.2, 56.4, 95.3, 111.0, 115.2, 126.8, 130.1, 146.9, 155.0, 190.8; HRMS (ESI-TOF) *m/z*: $[M + H]^+$ calcd for $C_{10}H_{13}O_4$, 197.0808; found, 197.0812.

(*E*)-3-(3-Hydroxy-4-methoxyphenyl)acrylaldehyde (18)

By a procedure identical with that described for synthesis of **S2** from **S1**, the benzaldehyde **S16** (201 mg, 1.02 mmol) was converted into a crude **S17** (90.0 mg), which was used without further purification. Then, by a procedure similar to that described for synthesis of **10** from **S2**, the crude acetal **S17** (41.8 mg) was converted into the aldehyde **18** (13.4 mg, 16% yield, 2 steps). Column chromatography: silica gel (gradient 6% to 40% EtOAc in *n*-hexane): yellow solid; mp 149–150 °C; IR (neat cm^{-1}): 1660 (C=O); ^1H NMR (500 MHz, $CDCl_3$): δ 3.96 (s, 3H), 5.67 (s, 1H), 6.59 (dd, J = 16.0, 7.4 Hz, 1H), 6.89 (d, J = 8.6 Hz, 1H), 7.10 (dd, J = 8.6, 2.3 Hz, 1H), 7.17 (d, J = 2.3 Hz, 1H), 7.38 (d, J = 16.0 Hz, 1H), 9.66 (d, J = 7.4 Hz, 1H); $^{13}C\{^1H\}$ NMR (150 MHz, DMSO-d_6) δ 56.1, 110.6, 113.4, 122.5, 127.0, 127.7, 146.0, 149.3, 153.0, 193.8; HRMS (ESI-TOF) *m/z*: $[M + H]^+$ calcd for $C_{10}H_{11}O_3$, 179.0703; found, 179.0708. The purity of **18** was >99% as determined by HPLC.

4-(Methoxymethoxy)-3-(3-methylbut-2-en-1-yl)benzaldehyde (S19)

By a procedure identical with that described for synthesis of **S16** from **S15**, the phenol **S18** (146 mg, 0.767 mmol) was converted into **S19** (120 mg, 67% yield). Column chromatography: silica gel (gradient 4% to 18% EtOAc in *n*-hexane): colorless oil; IR (neat cm^{-1}): 1689 (C=O); ^1H NMR (500 MHz, $CDCl_3$): δ 1.73 (s, 3H), 1.76 (s, 3H), 3.38 (d, J = 7.4 Hz, 2H), 3.49 (s, 3H), 5.26-5.32 (m, 3H), 7.17 (d, J = 8.0 Hz, 1H), 7.68-7.71 (m, 2H), 9.87 (s, 1H).;

$^{13}C\{^1H\}$ NMR (125 MHz, $CDCl_3$): δ 17.8, 25.8, 28.5, 56.3, 94.0, 113.2, 121.4, 130.2, 130.4, 130.6, 131.6, 133.4, 160.0, 191.3; HRMS (ESI-TOF) *m/z*: $[M + H]^+$ calcd for $C_{14}H_{19}O_3$, 235.1329; found, 235.1330.

(*E*)-3-[4-Hydroxy-3-(3-methylbut-2-en-1-yl)phenyl]acrylaldehyde (19)

By a procedure identical with that described for synthesis of **S2** from **S1**, the benzaldehyde **S19** (118 mg, 0.504 mmol) was converted into a crude **S20** (52.0 mg), which was used without further purification. Then, by a procedure similar to that described for synthesis of **10** from **S2**, the crude acetal **S20** (52.0 mg) was converted into the aldehyde **19** (26.7 mg, 24% yield, 2 steps). Column chromatography: silica gel (gradient 6% to 35% EtOAc in *n*-hexane): pale yellow solid; ^1H NMR (500 MHz, $CDCl_3$) δ 1.793–1.804 (m, 6H), 3.39 (d, J = 6.9 Hz, 2H), 5.30–5.33 (m, 1H), 5.53 (s, 1H), 6.60 (dd, J = 16.0, 8.0 Hz, 1H), 6.85 (d, J = 8.0 Hz, 1H), 7.34–7.37 (m, 2H), 7.40 (d, J = 16.0 Hz, 1H), 9.64 (d, J = 8.0 Hz, 1H); $^{13}C\{^1H\}$ NMR (150 MHz, $CDCl_3$): δ 17.9, 25.8, 29.2, 116.3, 120.9, 125.9, 126.6, 128.0, 128.6, 130.6, 135.4, 154.0, 157.7, 194.3; HRMS (ESI-TOF) *m/z*: $[M + H]^+$ calcd for $C_{14}H_{17}O_2$, 217.1223; found, 217.1227. The purity of **19** was 96% as determined by HPLC.

(*E*)-3-(4-Hydroxy-3,5-dimethoxyphenyl)acrylaldehyde (20)

By a procedure identical with that described for synthesis of **S2** from **S1**, the benzaldehyde **S21** (223 mg, 0.986 mmol) was converted into a crude **S22** (306 mg), which was used without further purification. Then, by a procedure similar to that described for synthesis of **10** from **S2**, the crude acetal **S22** (148 mg) was converted into the aldehyde **20** (104 mg, quant, 2 steps). Column chromatography: silica gel (gradient 12% to 75% EtOAc in *n*-hexane): yellow oil; IR (neat cm^{-1}): 3357 (OH), 1669 (C=O); ^1H NMR (500 MHz, $CDCl_3$): δ 3.95 (s, 6H), 5.89 (s, 1H), 6.61 (dd, J = 15.8, 7.8 Hz, 1H), 6.82 (s, 2H), 7.39 (d, J = 15.8 Hz, 1H), 9.66 (d, J = 7.8 Hz, 1H); $^{13}C\{^1H\}$ NMR (150 MHz, $CDCl_3$): δ 56.3 (2C), 105.5 (2C), 125.5, 126.7, 138.0, 147.3 (2C), 153.2, 193.5; HRMS (ESI-TOF) *m/z*: $[M - H]^-$ calcd for $C_{11}H_{11}O_4$, 207.0663; found, 207.0667. The purity of **20** was >99% as determined by HPLC.

(*E*)-3-(7-Methoxybenzo[*d*][1,3]dioxol-5-yl)acrylaldehyde (21).

By a procedure identical with that described for synthesis of **S2** from **S1**, the benzaldehyde **S23** (85.2 mg, 0.473 mmol) was converted into a crude **S24** (101 mg), which was used without further purification. Then, to a stirred solution of **S24** (25.3 mg) in THF (0.180 mL) was added aqueous solution of HCl (1 M; 0.300 mL). After being stirred for 1.5 h at room temperature, the mixture was diluted with saturated aqueous solution of $NaHCO_3$. The whole was extracted with EtOAc, washed with H_2O and brine, dried over $MgSO_4$, and filtered. The filtrate was concentrated *in vacuo* to give **21** (20.8 mg, 86% yield, 2 steps): pale yellow solid; ^1H NMR (500 MHz, $CDCl_3$) δ 3.95 (s, 3H), 6.06 (s, 2H), 6.57 (dd, J = 15.5, 7.7 Hz, 1H), 6.75 (d, J = 1.7 Hz, 1H), 6.79 (d, J = 1.7 Hz, 1H), 7.35 (d, J = 15.5 Hz, 1H), 9.66 (d, J = 7.7 Hz, 1H); $^{13}C\{^1H\}$ NMR (150 MHz, $CDCl_3$) δ 56.7, 101.8, 102.2, 109.6, 127.3, 128.8, 138.2, 143.8, 149.5, 152.6, 193.5; HRMS (ESI-TOF) *m/z*: $[M + H]^+$ calcd for $C_{11}H_{11}O_4$, 207.0652; found, 207.0655. The purity of **21** was >99% as determined by HPLC.

(*E*)-3-(4,7-Dimethoxybenzo[*d*][1,3]dioxol-5-yl)acrylaldehyde (22).

By a procedure identical with that described for synthesis of **S2** from **S1**, the benzaldehyde **S25** (106 mg, 0.504 mmol) was converted into a crude **S26** (79.8 mg), which was used without further purification. Then, by a procedure

similar to that described for synthesis of **21** from **S24**, the crude acetal **S26** (57.1 mg) was converted into the aldehyde **22** (29.5 mg, 34% yield, 2 steps). Column chromatography: silica gel (gradient 6% to 25% EtOAc in *n*-hexane): white solid; mp 142–143 °C; IR (neat cm^{-1}): 1682 (C=O); ^1H NMR (500 MHz, $CDCl_3$) δ 3.89 (s, 3H), 4.01 (s, 3H), 6.06 (s, 2H), 6.65 (dd, J = 16.0, 7.7 Hz, 1H), 6.75 (s, 1H), 7.72 (d, J = 16.0 Hz, 1H), 9.66 (d, J = 7.7 Hz, 1H); $^{13}C\{^1H\}$ NMR (150 MHz, $CDCl_3$) δ 56.7, 60.3, 102.4, 106.5, 119.9, 127.6, 138.1, 138.5, 139.5, 140.1, 147.5, 194.2; HRMS (ESI-TOF) *m/z*: $[M + H]^+$ calcd for $C_{12}H_{13}O_5$, 237.0757; found, 237.0753. The purity of **22** was >99% as determined by HPLC.

(2*E*,4*E*)-5-(4-Hydroxy-3-methoxyphenyl)penta-2,4-dienal (25)

By a procedure identical with that described for synthesis of **S2** from **S1**, the benzaldehyde **S27** (292 mg, 1.00 mmol) was converted into a crude **S28** (225 mg), which was used without further purification. Then, by a procedure similar to that described for synthesis of **10** from **S2**, the crude acetal **S28** (109 mg) was converted into the aldehyde **25** (70.6 mg, 71% yield, 2 steps). Column chromatography: silica gel (gradient 6% to 40% EtOAc in *n*-hexane): yellow oil; IR (neat cm^{-1}): 3357 (OH), 1671 (C=O); ^1H NMR (500 MHz, $CDCl_3$) δ 3.95 (s, 3H), 5.96 (s, 1H), 6.24 (dd, J = 15.2, 8.0 Hz, 1H), 6.86 (dd, J = 15.2, 11.2 Hz, 1H), 6.91–6.97 (m, 2H), 7.02–7.05 (m, 2H), 7.23–7.28 (m, 1H), 9.59 (d, J = 8.0 Hz, 1H); $^{13}C\{^1H\}$ NMR (150 MHz, $CDCl_3$) δ 56.0, 108.6, 114.8, 122.6, 124.0, 128.3, 130.6, 142.7, 146.8, 147.5, 152.7, 193.7; HRMS (ESI-TOF) *m/z*: $[M + H]^+$ calcd for $C_{12}H_{13}O_3$, 205.0859; found, 205.0856. The purity of **25** was 99% as determined by HPLC.

(*E*)-4-(4-Hydroxy-3-methoxyphenyl)but-3-en-2-one (26)

The solution of **24** (157 mg, 1.03 mmol) and (acetylmethylene)triphenylphosphorane (770 mg, 2.42 mmol) in toluene (2.00 mL) was refluxed for 1 h under Ar. After concentration *in vacuo*, the residue was purified by flash chromatography over silica gel with a gradient of 10% to 95% EtOAc in *n*-hexane to afford **26** (192 mg, 62% yield): white solid; mp 127–128 °C; IR (neat cm^{-1}): 3340 (OH), 1664 (C=O); ^1H NMR (500 MHz, $CDCl_3$) δ 2.37 (s, 3H), 3.93 (s, 3H), 6.15 (s, 1H), 6.59 (d, J = 16.0 Hz, 1H), 6.93 (d, J = 8.0 Hz, 1H), 7.06 (d, J = 2.3 Hz, 1H), 7.09 (dd, J = 8.0, 2.0 Hz, 1H), 7.45 (d, J = 16.0 Hz, 1H); $^{13}C\{^1H\}$ NMR (150 MHz, $CDCl_3$): δ 27.1, 55.8, 109.3, 114.8, 123.4, 124.7, 126.6, 144.0, 146.9, 149.3, 198.7; HRMS (ESI-TOF) *m/z*: $[M - H]^-$ calcd for $C_{11}H_{11}O_3$, 191.0714; found, 191.0716. The purity of **26** was >99% as determined by HPLC.

(*E*)-3-(3-Methoxyphenyl)acrylaldehyde (29)

By a procedure identical with that described for synthesis of **S2** from **S1**, the benzaldehyde **S29** (136 mg, 1.00 mmol) was converted into a crude **S30** (230 mg), which was used without further purification. Then, by a procedure similar to that described for synthesis of **10** from **S2**, the crude acetal **S30** (49.0 mg) was converted into the aldehyde **29** (34.9 mg, quant, 2 steps). Column chromatography: silica gel (gradient 6% to 35% EtOAc in *n*-hexane): colorless oil; IR (neat cm^{-1}): 3357 (OH), 1676 (C=O); ^1H NMR (500 MHz, $CDCl_3$) δ 3.85 (s, 3H), 6.71 (dd, J = 16.0, 8.0 Hz, 1H), 6.99–7.01 (m, 1H), 7.08–7.09 (m, 1H), 7.16–7.18 (m, 1H), 7.36 (dd, J = 8.0 Hz, 1H), 7.46 (d, J = 16.0 Hz, 1H), 9.71 (d, J = 8.0 Hz, 1H); $^{13}C\{^1H\}$ NMR (150 MHz, $CDCl_3$) δ 55.3, 113.2, 117.1, 121.2, 128.8, 130.1, 135.3, 152.7, 159.9, 193.7; HRMS (ESI-TOF) *m/z*: $[M + Na]^+$ calcd for $C_{10}H_{10}NaO_2$, 185.0573; found, 185.0576. The purity of **29** was >99% as determined by HPLC.

(*E*)-3-(2-Hydroxy-5-methoxyphenyl)acrylaldehyde (30)

By a procedure identical with that described for synthesis of **S2** from **S1**, the benzaldehyde **S31** (189 mg, 0.963 mmol) was converted into a crude **S32** (205 mg), which was used without further purification. Then, by a procedure similar to that described for synthesis of **10** from **S2**, the crude acetal **S32** (81.4 mg) was converted into the aldehyde **30** (32.9 mg, 48% yield, 2 steps). Column chromatography: silica gel (gradient 12% to 35% EtOAc in *n*-hexane): yellow solid; mp 124–125 °C; IR (neat cm^{-1}): 3281 (OH), 1657 (C=O); ^1H NMR (500 MHz, $CDCl_3$): δ 3.80 (s, 3H), 5.46 (s, 1H), 6.79 (d, J = 8.6 Hz, 1H), 6.85 (dd, J = 16.0, 8.0 Hz, 1H), 6.90 (dd, J = 8.6, 2.9 Hz, 1H), 7.02 (d, J = 2.9 Hz, 1H), 7.80 (d, J = 16.0 Hz, 1H), 9.70 (d, J = 8.0 Hz, 1H); $^{13}C\{^1H\}$ NMR (125 MHz, $CDCl_3$): δ 55.8, 112.8, 117.4, 119.4, 121.6, 129.0, 149.0, 149.7, 153.6, 195.3; HRMS (ESI-TOF) *m/z*: $[M + H]^+$ calcd for $C_{10}H_{11}O_3$, 179.0703; found, 179.0700. The purity of **30** was 99% as determined by HPLC.

2-[4-(Methoxymethoxy)-3-nitrostyryl]-1,3-dioxolane (S34)

By a procedure identical with that described for synthesis of **S2** from **S1**, the benzaldehyde **S33** (1.68 g, 7.96 mmol) was converted into **S34** (2.31 g, quant) as an isomeric mixture (*E*:*Z* = 55:45).. Column chromatography: amine silica gel (*n*-hexane:EtOAc = 3:1), followed by silica gel (*n*-hexane:EtOAc = 3:1): pale yellow amorphous; IR (neat cm^{-1}): 1532, 1358 (NO_2); ^1H NMR (500 MHz, $CDCl_3$) δ 3.52–3.53 (m, 3H), 3.92–3.98 (m, 2H), 4.05–4.10 (m, 2H), 5.29–5.31 (m, 2H), 5.42-5.47 (m, 1H), 5.79 (dd, J = 11.7, 7.2 Hz, 0.45H), 6.14 (dd, J = 16.0, 5.7 Hz, 0.55H), 6.70–6.73 (m, 1H), 7.28–7.31 (m, 1H), 7.53–7.56 (m, 1H), 7.85–7.87 (m, 1H); $^{13}C\{^1H\}$ NMR (150 MHz, $CDCl_3$): δ 56.8 (2C), 65.2 (2C), 65.3 (2C), 95.19, 95.24, 99.3, 103.3, 116.9, 117.3, 123.6, 125.6, 126.5, 129.2, 129.5, 129.9, 131.86, 131.90, 132.7, 134.3, 140.5, 140.6, 149.7, 150.1; HRMS (ESI-TOF) *m/z*: $[M + H]^+$ calcd for $C_{13}H_{16}NO_6$, 282.0972; found, 282.0977.

(*E*)-3-[3-(Dimethylamino)-4-hydroxyphenyl]acrylaldehyde (31)

To a stirred solution of **S34** (434 mg, 1.54 mmol) in EtOH (59.1 mL) were added AcOH (5.91 mL) and zinc dust (1.03 g, 15.7 mmol) successively at 0 °C. After being stirred for 1 h at 0 °C under Ar, the mixture was filtered through cerite and washed with EtOAc. The filtrate was diluted with aqueous solution of 2 M NaOH. The whole was extracted with EtOAc, washed with saturated aqueous solution of $NaHCO_3$, and dried over $MgSO_4$. After concentration *in vacuo*, the residue was purified by flash chromatography over silica gel with a gradient of 12% to 65% EtOAc in *n*-hexane to give a crude **S35** as a yellow oil (211 mg), which was used without further purification. Then, to a stirred solution of **S35** (49.5 mg), paraformaldehyde (32.3 mg, 1.08 mmol) and $NaBH_3CN$ (67.9 mg, 1.08 mmol) in THF (813 μL) was slowly added AcOH (61.8 μL). After being stirred for 4 h at 50 °C under Ar, the mixture was neutralized with aqueous solution of $NaHCO_3$, diluted with Et_2O, washed with saturated aqueous solution of $NaHCO_3$ and dried over $MgSO_4$. After concentration *in vacuo*, the residue was purified by flash chromatography over silica gel with a gradient of 6% to 40% EtOAc in *n*-hexane to afford **S36** as a colorless oil (14.4 mg), which was used without further purification. Then, by a procedure similar to that described for synthesis of **10** from **S2**, the crude acetal **S36** (14.4 mg) was converted into the aldehyde **31** (8.40 mg, 12% yield, 3 steps). Column chromatography: silica gel (gradient 12% to 50% EtOAc in *n*-hexane): yellow oil; IR (neat cm^{-1}): 3299 (OH), 1666 (C=O); ^1H NMR (500 MHz, $CDCl_3$) δ 2.69 (s, 6H), 6.60 (dd, J = 16.0, 8.0 Hz, 1H), 6.99 (d, J = 8.6 Hz, 1H), 7.31 (dd, J = 8.6, 2.0 Hz, 1H), 7.38–7.41 (m, 2H), 9.65 (d, J = 8.0 Hz, 1H); $^{13}C\{^1H\}$ NMR (125 MHz, $CDCl_3$) δ 45.1

(2C), 114.7, 121.0, 126.2, 126.4, 127.7, 141.3, 153.1, 154.6, 193.7; HRMS (ESI-TOF) *m/z*: $[M + H]^+$ calcd for $C_{11}H_{14}NO_2$, 192.1019; found, 192.1017. The purity of **31** was 99% as determined by HPLC.

2,5-Dimethoxy-4-(methoxymethoxy)benzaldehyde (S39)

The solution of **S37** (818 mg, 2.80 mmol), CuI (56.1 mg, 0.295 mmol), 1,10-phenanthroline (101 mg, 0.560 mmol) and KOH (616 mg, 9.33 mmol) in H_2O/DMSO (1:1; 4.48 mL) was purged with Ar. After being stirred for 10 min at room temperature, the reaction mixture was stirred for 11 h at 100 °C. Then, the mixture was acidified with aqueous solution of 1 M HCl, diluted with EtOAc, filtered through Kiriyama funnel and washed with EtOAc. The filtrate was washed with H_2O and brine, and dried over $MgSO_4$. After concentration *in vacuo*, the residue was purified by flash chromatography over silica gel with a gradient of 6% to 40% EtOAc in *n*-hexane to give **S38** (89.6 mg). Then, by a procedure identical with that described for synthesis of **S16** from **S15**, the phenol **S38** (76.1 mg, 0.418 mmol) was converted into **S39** (47.1 mg, 45% yield, 2 steps). Column chromatography: silica gel (gradient 5% to 35% EtOAc in *n*-hexane), followed by silica gel (*n*-hexane:EtOAc = 5:1): pale yellow solid; mp 72–73 °C; IR (neat cm^{-1}): 1672 (C=O); ^1H NMR (500 MHz, $CDCl_3$) δ 3.54 (s, 3H), 3.89 (s, 3H), 3.90 (s, 3H), 5.33 (s, 2H), 6.85 (s, 1H), 7.36 (s, 1H), 10.34 (s, 1H); $^{13}C\{^1H\}$ NMR (150 MHz, $CDCl_3$) δ 56.2, 56.3, 56.6, 95.2, 99.8, 109.5, 118.4, 143.9, 153.4, 158.2, 188.3; HRMS (ESI-TOF) *m/z*: $[M + H]^+$ calcd for $C_{11}H_{15}O_5$, 227.0914; found, 227.0912.

(*E*)-3-(4-Hydroxy-2,5-dimethoxyphenyl)acrylaldehyde (32)

By a procedure identical with that described for synthesis of **S2** from **S1**, the benzaldehyde **S39** (33.4 mg, 0.148 mmol) was converted into a crude **S40** (42.3 mg), which was used without further purification. Then, by a procedure similar to that described for synthesis of **10** from **S2**, the crude acetal **S40** (42.3 mg) was converted into the aldehyde **32** (33.6 mg, quant, 2 steps). Column chromatography: silica gel (gradient 12% to 45% EtOAc in *n*-hexane): yellow solid; mp 115–116 °C; IR (neat cm^{-1}): 3299 (OH), 1663 (C=O); ^1H NMR (500 MHz, $CDCl_3$) δ 3.86 (s, 3H), 3.90 (s, 3H), 6.03 (s, 1H), 6.59 (s, 1H), 6.63 (dd, J = 15.5, 7.7 Hz, 1H), 7.02 (s, 1H), 7.81 (d, J = 15.5 Hz, 1H), 9.64 (d, J = 7.7 Hz, 1H); $^{13}C\{^1H\}$ NMR (150 MHz, $CDCl_3$) δ 56.1, 56.4, 99.3, 109.7, 114.3, 126.2, 140.9, 148.1, 150.3, 154.5, 194.4; HRMS (ESI-TOF) *m/z*: $[M + H]^+$ calcd for $C_{11}H_{13}O_4$, 209.0808; found, 209.0806. The purity of **32** was >99% as determined by HPLC.

5-Bromo-3-methoxy-2-(methoxymethoxy)pyridine (S43)

The mixture of **S41** (512 mg, 2.30 mmol), acetohydroxamic acid (540 mg, 7.19 mmol) and K_2CO_3 (1.61 g, 11.6 mmol) in DMSO was stirred at 80 °C under Ar. After being stirred for 15.5 h at this temperature under Ar, the mixture was neutralized with aqueous solution of HCl (2 M), diluted with EtOAc, washed with H_2O and brine, and dried over $MgSO_4$. After concentration *in vacuo*, the residue was purified by flash chromatography over silica gel with $CHCl_3$–MeOH (15:1) to afford **S42** (248 mg) , which was used without further purification. To a stirred solution of **S42** (205 mg) in DMF (10.0 mL) were added NaH (160 mg, 4.00 mmol) and MOMCl (304 μL, 4.00 mmol) successively. After being stirred for 4 h at 0 °C under Ar, the mixture was diluted with saturated aqueous solution of NH_4Cl. The whole was extracted with EtOAc, washed with H_2O and brine, and dried over $MgSO_4$. After concentration *in vacuo*, the residue was purified by flash chromatography over silica gel with a gradient of 10% to 75% EtOAc in *n*-hexane to give **S43** (91.8 mg, 19% yield, 2 steps): white solid; mp 56–57 °C; ^1H NMR (500 MHz,

$CDCl_3$) δ 3.54 (s, 3H), 3.89 (s, 3H), 5.57 (s, 2H), 7.20 (d, J = 1.7 Hz, 1H), 7.80 (d, J = 1.7 Hz, 1H); $^{13}C\{^1H\}$ NMR (125 MHz, $CDCl_3$) δ 56.0, 57.3, 92.1, 112.0, 121.1, 137.5, 144.6, 151.8; HRMS (ESI-TOF) *m/z*: $[M + H]^+$ calcd for $C_8H_{11}BrNO_3$, 247.9917; found, 247.9917.

5-Methoxy-6-(methoxymethoxy)nicotinaldehyde (S44)

To a stirred solution of **S43** (205 mg, 0.826 mmol) in THF (2.37 mL) at −78 °C was added *n*-BuLi (1.32 M; 657 µL, 0.867 mmol). After the mixture was stirred for 1 h at −78 °C, DMF (128 µL, 1.65 mmol) was added and the stirring was continued for 1.5 h at −78 °C. The mixture was quenched with saturated aqueous solution of $NaHCO_3$. The whole was extracted with EtOAc, washed with H_2O and brine, and dried over $MgSO_4$. After concentration *in vacuo*, the residue was purified by flash chromatography over silica gel with a gradient of 6% to 40% EtOAc in *n*-hexane to give **S44** (126 mg, 77% yield). Column chromatography: silica gel (gradient 6% to 40% EtOAc in *n*-hexane): white amorphous; IR (neat cm^{-1}): 1690 (C=O); ^1H NMR (500 MHz, $CDCl_3$) δ 3.59 (s, 3H), 3.95 (s, 3H), 5.69 (s, 2H), 7.54 (d, J = 1.7 Hz, 1H), 8.22 (d, J = 1.7 Hz, 1H), 9.95 (s, 1H); $^{13}C\{^1H\}$ NMR (125 MHz, $CDCl_3$): δ 56.0, 57.7, 92.8, 113.7, 128.0, 144.2, 144.9, 157.0, 189.6; HRMS (ESI-TOF) *m/z*: $[M + H]^+$ calcd for $C_9H_{12}NO_4$, 198.0761; found, 198.0763.

(*E*)-3-(5-Methoxy-6-oxo-1,6-dihydropyridin-3-yl)acrylaldehyde (33)

By a procedure identical with that described for synthesis of **S2** from **S1**, the benzaldehyde **S44** (116 mg, 0.588 mmol) was converted into a crude **S45** (130 mg), which was used without further purification. Then, by a procedure similar to that described for synthesis of **10** from **S2**, the crude acetal **S45** (51.4 mg) was converted into the aldehyde **33** (23.2 mg, 56% yield, 2 steps): white solid; mp 294–295 °C; IR (neat cm^{-1}): 1739 (C=O); ^1H NMR (600 MHz, DMSO) δ 3.77 (s, 3H), 6.70 (dd, J = 15.5, 7.5 Hz, 1H), 7.20 (d, J = 2.7 Hz, 1H), 7.51–7.53 (m, 1H), 9.54 (d, J = 7.5 Hz, 1H); $^{13}C\{^1H\}$ NMR (150 MHz, CD_3OD): δ 55.7, 109.8, 113.6, 125.2, 131.4, 149.5, 150.3, 157.4, 193.6; HRMS (ESI-TOF) *m/z*: $[M + H]^+$ calcd for $C_9H_9NO_3$, 180.0655; found, 180.0652. The purity of **33** was 98% as determined by HPLC.

Materials

The 5-OP-RU in DMSO (10 mM) was freshly prepared by the incubation of a mixture of 5-A-RU in DMSO (20 mM) and methylglyoxal in DMSO (50 mM) for 18 h. Acetyl-6-formylpterin (Ac-6-FP) was purchased from Cayman Chemical, Michigan, USA.

Cell lines and cell culture

Human MR1-overexpressing HeLa cell line was established by the retroviral gene transduction of human MR1 and human CD8α as described previously.[51] A MAIT cell line was generated by the retroviral gene transduction of MAIT-αβTCRs into a murine thymoma TG40 (negative for TCR), as described previously.[52] HeLa cells and HEK293 cells were cultured in DMEM medium (Sigma-Aldrich) supplemented with 10% FBS (Sigma-Aldrich) and 1% penicillin/streptomycin (Wako Pure Chemical Industries). TG40 cells were cultured in RPMI-1640 medium (nacalai tesque) supplemented with 10% FBS and 1% penicillin/streptomycin. In the T cell activation assay, MR1 translocation assay and MR1 specificity assay, both cell lines were cultured in RPMI-1640 medium without folic

acid, and with 10% FBS and 1% penicillin/streptomycin (assay medium). All cell lines were maintained at 37°C in a humidified 5% CO_2 atmosphere.

HEK 293 cells expressing HiBiT-tagged human MR1

cDNAs corresponding to human β_2m and human MR1, linked through a glycine-serine flexible linker, were cloned in frame with an N-terminal HiBiT tag and a His tag into the pCAG-Hyg PA tag (Wako Pure Chemical Industries). HEK 293 cells were transfected by lipofection using ScreenFect A (Wako Pure Chemical Industries) and selected by blasticidin S. Sequence of the construct used for expression of HiBiT-tagged MR1 in HEK293 cell line is as follows.

MYRMQLLSCIALSLALVTNSHHHHHHVSGWRLFKKISGGGGSIQRTPKIQVYSRHPAENGKSNFLNCYVS
GFHPSDIEVDLLKNGERIEKVEHSDLSFSKDWSFYLLYYTEFTPTEKDEYACRVNHVTLSQPKIVKWDRD
MGGGGSGGSGSGGGGSRTHSLRYFRLGVSDPIHGVPEFISVGYVDSHPITTYDSVTRQKEPRAPWMAENL
APDHWERYTQLLRGWQQMFKVELKRLQRHYNHSGSHTYQRMIGCELLEDGSTTGFLQYAYDGQDFLIF
NKDTLSWLAVDNVAHTIKQAWEANQHELLYQKNWLEEECIAWLKRFLEYGKDTLQRTEPPLVRVNRKET
FPGVTALFCKAHGFYPPEIYMTWMKNGEEIVQEIDYGDILPSGDGTYQAWASIELDPQSSNLYSCHVEHC
GVHMVLQVPQESETIPLVMKAVSGSIVLVIVLAGVGVLVWRRRPREQNGAIYLPTPDRGVAMPGAEDDV
V

Screening with Nano-Glo®HiBiT technology

HEK.HiBiT-hMR1 cells (3.0×10^4 cells) were incubated for 3 h in 20 μL medium (DMEM without phenol red, and with 2% FBS and 1% penicillin/streptomycin) in 384-well plates. Then, each compound was added, followed by 8 h incubation at 37°C. After plates were cooled to room temperature, LgBiT and a luminescent substrate (Promega) were added. After incubation for 10 min at room temperature, epiluminescence was measured using the EnVision plate reader (PerkinElmer).

T cell activation assay

HeLa.hMR1 cells (4.5×10^4 cells) were co-incubated with TG40.MAIT-TCR cells (1.8×10^5 cells) for 24 h in 200 μL assay medium with various ligands at 37°C. The cells were subsequently labeled with PE-conjugated anti-mouse CD3 (BioLegend), APC-conjugated anti-mouse CD69 (BioLegend) and propidium iodide (PI), followed by Gallios flow cytometry analysis (Beckman Coulter, California, USA). Data were analyzed with Kaluza software (Beckman Coulter, v2.1). The activation of TG40 cells was evaluated by an increase in the cell surface levels of CD69.

MR1 translocation assay

HeLa.hMR1 cells (1.5×10^5 cells) were incubated for 8 h in 200 μL assay medium with various ligands at 37°C. The cells were subsequently labeled with PE-conjugated anti-human MR1 (BioLegend) and PI, followed by Gallios flow cytometry analysis (Beckman Coulter). Data were analyzed with Kaluza software (Beckman Coulter, v2.1).

Competition assay

HeLa.hMR1 cells (4.5×10^4 cells) were incubated for 30 min in 100 μL medium (RPMI-1640 without folic acid)

with various ligands (10 μM) at 37°C. Then, freshly prepared 5-OP-RU (0.1 nM) and TG40.MAIT-TCR cells (1.8×10^5 cells) were added. After 24 h incubation at 37°C, the cells were labeled with PE-conjugated anti-mouse CD3 (BioLegend, California, USA), APC-conjugated anti-mouse CD69 (BioLegend) and propidium iodide (PI), followed by Gallios flow cytometry analysis (Beckman Coulter, California, USA). Data were analyzed with Kaluza software (Beckman Coulter, v2.1). The activation of TG40 cells was evaluated by an increase in the cell surface levels of CD69.

MR1 specificity assay

HeLa.hMR1 cells (1.5×10^5 cells) were incubated for 8 h in 200 μL assay medium with various ligands at 37°C. The cells were subsequently labeled with PE-conjugated anti-human MR1 (BioLegend), APC-conjugated anti-HLA-A/B/C antibody (Biolegend) and PI, followed by Gallios flow cytometry analysis (Beckman Coulter). Data were analyzed with Kaluza software (Beckman Coulter, v2.1).

Binding mode study

The binding mode of the MR1-ligand complexes was analyzed using the Molecular Operating Environment (MOE) with the X-ray crystal structure of the MR1-ligand (6-FP) complex (PDB: 4GUP) as a template. The protein structure was preprocessed and optimized using the MOE QuickPrep command with the default settings. After modifying the ligand structure to coniferyl aldehyde derivatives, energy minimization calculations of the complex structures were performed with the Amber10:EHT force field. The minimization process of the residues within 8 Å around the ligand was carried out to predict the binding mode.

ASSOCIATED CONTENT

Supporting Information.

The Supporting Information is available free of charge on the ACS Publications website at DOI:

AUTHOR INFORMATION

Corresponding Authors

* E-mail: hohno@pharm.kyoto-u.ac.jp

* E-mail: sinuki@pharm.kyoto-u.ac.jp

ORCID

Akira Hattori: 0000-0001-5509-2326

Shinya Oishi: 0000-0002-2833-2539

Norihito Arichi: 0000-0003-3618-4959

Hideaki Kakeya: 0000-0002-4293-7331

Sho Yamasaki: 0000-0002-5184-6917

Hiroaki Ohno: 0000-0002-3246-4809

Shinsuke Inuki: 0000-0002-7525-1280

Notes

The authors declare no competing financial interest.

Acknowledgment

This work was supported by JSPS KAKENHI (Grant Numbers JP20K06938, JP20H04773, 22H05183 and A22H051830), AMED under grant number JP21gm1010007, JP21ak0101070 and 223fa727001h0001, and Research Support Project for Life Science and Drug Discovery (Basis for Supporting Innovative Drug Discovery and Life Science Research (BINDS)) from AMED under grant number JP22ama121042. T.M. is grateful for JSPS Research Fellowships for Young Scientists.

References

(1) Ussher, J. E.; Klenerman, P.; Willberg, C. B. Mucosal-Associated Invariant T-Cells: New Players in Anti-Bacterial Immunity. *Front. Immunol.* **2014**, *5*, 450.

(2) Godfrey, D. I.; Uldrich, A. P.; McCluskey, J.; Rossjohn, J.; Moody, D. B. The Burgeoning Family of Unconventional T Cells. *Nat. Immunol.* **2015**, *16*, 1114–1123.

(3) Godfrey, D. I.; Koay, H.-F.; McCluskey, J.; Gherardin, N. A. The Biology and Functional Importance of MAIT Cells. *Nat. Immunol.* **2019**, *20*, 1110–1128.

(4) Legoux, F.; Salou, M.; Lantz, O. MAIT Cell Development and Functions: the Microbial Connection. *Immunity* **2020**, *53*, 710–723.

(5) Dusseaux, M.; Martin, E.; Serriari, N.; Péguillet, I.; Premel, V.; Louis, D.; Milder, M.; Le Bourhis, L.; Soudais, C.; Treiner, E.; Lantz, O. Human MAIT Cells Are Xenobiotic-Resistant, Tissue-Targeted, CD161hi IL-17-Secreting T Cells. *Blood* **2011**, *117*, 1250–1259.

(6) Gold, M. C.; Cerri, S.; Smyk-Pearson, S.; Cansler, M. E.; Vogt, T. M.; Delepine, J.; Winata, E.; Swarbrick, G. M.; Chua, W.-J.; Yu, Y. Y. L.; Lantz, O.; Cook, M. S.; Null, M. D. Human Mucosal Associated Invariant T Cells Detect Bacterially Infected Cells. *PLoS Biol.* **2010**, *8*, e1000407.

(7) Meierovics, A. I.; Cowley, S. C. MAIT Cells Promote Inflammatory Monocyte Differentiation into Dendritic Cells During Pulmonary Intracellular Infection. *J. Exp. Med.* **2016**, *213*, 2793–2809.

(8) Yan, J.; Allen, S.; McDonald, E.; Das, I.; Mak, J. Y. W.; Liu, L.; Fairlie, D. P.; Meehan, B. S.; Chen, Z.; Corbett,

A. J.; Varelias, A.; Smyth, M. J.; Teng, M. W. L. MAIT Cells Promote Tumor Initiation, Growth, and Metastases via Tumor MR1. *Cancer Discovery* **2020**, *10*, 124–141.

(9) Toubal, A.; Nel, I.; Lotersztajn, S.; Lehuen, A. Mucosal-Associated Invariant T Cells and Disease. *Nat. Rev. Immunol.* **2019**, *19*, 643–657.

(10) Chiba, A.; Tajima, R.; Tomi, C.; Miyazaki, Y.; Yamamura, T.; Miyake, S. Mucosal-Associated Invariant T Cells Promote Inflammation and Exacerbate Disease in Murine Models of Arthritis. *Arthritis Rheum* **2012**, *64*, 153–161.

(11) Marwaha, A.; Leung, N. J.; McMurchy, A. N.; Levings, M. K. TH17 Cells in Autoimmunity and Immunodeficiency: Protective or Pathogenic? *Front. Immunol.* **2012**, *3*, 129.

(12) Pankhurst, T. E.; Buick, K. H.; Lange, J. L.; Marshall, A. J.; Button, K. R.; Palmer, O. R.; Farrand, K. J.; Stewart, I. F. N.; Bird, T.; Mason, N. C.; Compton, B. J.; Comoletti, D.; Salio, M.; Cerundolo, V.; Painter, G. F.; Hermans, I. F.; Connor, L. M. MAIT Cells Activate Dendritic Cells to Promote T Follicular Helper Cell Differentiation and Humoral Immunity. *bioRxiv* **2022** DOI: 10.1101/2022.03.31.486638.

(13) Murayama, G.; Chiba, A.; Suzuki, H.; Nomura, A.; Mizuno, T.; Kuga, T.; Nakamura, S.; Amano, H.; Hirose, S.; Yamaji, K.; Suzuki, Y.; Tamura, N.; Miyake, S. A Critical Role for Mucosal-Associated Invariant T Cells as Regulators and Therapeutic Targets in Systemic Lupus Erythematosus. *Front. Immunol.* **2019**, *10*, 2681.

(14) Kjer-Nielsen, L.; Patel, O.; Corbett, A. J.; Le Nours, J.; Meehan, B.; Liu, L.; Bhati, M.; Chen, Z.; Kostenko, L.; Reantragoon, R.; Williamson, N. A.; Purcell, A. W.; Dudek, N. L.; McConville, M. J.; O'Hair, R. A. J.; Khairallah, G. N.; Godfrey, D. I.; Fairlie, D. P.; Rossjohn, J.; McCluskey, J. MR1 Presents Microbial Vitamin B Metabolites to MAIT Cells. *Nature* **2012**, *491*, 717–723.

(15) Patel, O.; Kjer-Nielsen, L.; Le Nours, J.; Eckle, S. B. G.; Birkinshaw, R.; Beddoe, T.; Corbett, A. J.; Liu, L.; Miles, J. J.; Meehan, B.; Reantragoon, R.; Sandoval-Romero, M. L.; Sullivan, L. C.; Brooks, A. G.; Chen, Z.; Fairlie, D. P.; McCluskey, J.; Rossjohn, J. Recognition of Vitamin B Metabolites by Mucosal-Associated Invariant T Cells. *Nat. Commun.* **2013**, *4*, 2142.

(16) Corbett, A. J.; Eckle, S. B. G.; Birkinshaw, R. W.; Liu, L.; Patel, O.; Mahony, J.; Chen, Z.; Reantragoon, R.; Meehan, B.; Cao, H.; Williamson, N. A.; Strugnell, R. A.; Sinderen, D. V.; Mak, J. Y. W.; Fairlie, D. P.; Kjer-Nielsen, L.; Rossjohn, J.; McCluskey, J. T-Cell Activation by Transitory Neo-Antigens Derived from Distinct Microbial Pathways. *Nature* **2014**, *509*, 361–365.

(17) Keller, A. N.; Eckle, S. B. G.; Xu, W.; Liu, L.; Hughes, V. A.; Mak, J. Y. W.; Meehan, B. S.; Pediongco, T.; Birkinshaw, R. W.; Chen, Z.; Wang, H.; D'Souza, C.; Kjer-Nielsen, L.; Gherardin, N. A.; Godfrey, D. I.; Kostenko, L.; Corbett, A. J.; Purcell, A. W.; Fairlie, D. P.; McClusky, J.; Rossjohn, J. Drugs and Drug-Like Molecules Can Modulate the Function of Mucosal-Associated Invariant T Cells. *Nat. Immunol.* **2017**, *18*, 402–411.

(18) Salio, M.; Awad, W.; Veerapen, N.; Cerundolo, V. Ligand-Dependent Downregulation of MR1 Cell Surface Expression. *Prod. Natl. Acad. Sci. U.S.A.* **2020**, *117*, 10465–10475.

(19) Lepore, M.; Kalinichenko, A.; Calogero, S.; Kumar, P.; Paleja, B.; Schmaler, M.; Narang, V.; Zolezzi, F.; Poidinger, M.; Mori, L.; Libero, G. D. Functionally Diverse Human T Cells Recognize Non-Microbial Antigens Presented by MR1. *eLife* **2017**, *6*, e24476.

(20) Crowther, M. D.; Dolton, G.; Legut, M.; Caillaud, M. E.; Lloyd, A.; Attaf, M.; Galloway, S. A. E.; Rius, C.;

Farrell, C. P.; Szomolay, B.; Ager, A.; Parker, A. L.; Fuller, A.; Donia, M.; McCluskey, J.; Rossjohn, J.; Svane, I. M.; Phillips, J. D.; Sewell, A. K. Genome-Wide CRISPR–Cas9 Screening Reveals Ubiquitous T Cell Cancer Targeting via the Monomorphic MHC Class I-Related Protein MR1. *Nat. Immunol.* **2020**, *21*, 178–185.

(21) McWilliam, H. E. G.; Eckle, S. B. G.; Theodossis, A.; Liu, L.; Chen, Z.; Wubben, J. M.; Fairlie, D. P.; Strugnell, R. A.; Mintern, J. D.; McCluskey, J.; Rossjohn, J.; Villadangos, J. A. The Intracellular Pathway for the Presentation of Vitamin B-Related Antigens by the Antigen-Presenting Molecule MR1. *Nat. Immunol.* **2016**, *17*, 531–537.

(22) McWilliam, H. E. G.; Mak, J. Y. W.; Awad, W.; Zorkau, M.; Cruz-Gomez, C.; Lim, H. J.; Yan, Y.; Wormald, S.; Dagley, L. F.; Eckle, S. B. G.; Corbett, A. J.; Liu, H.; Li, S.; Reddiex, S. J. J.; Mintern, J. D.; Liu, L.; McCluskey, J.; Rossjohn, J.; Fairlie, D. P.; Villadangos, J. A. Endoplasmic Reticulum Chaperones Stabilize Ligand-Receptive MR1 Molecules for Efficient Presentation of Metabolite Antigens. *Prod. Natl. Acad. Sci. U.S.A.* **2020**, *117*, 24974–24985.

(23) McShan, A. C.; Devlin, C. A.; Papadaki, G. F.; Sun, Y.; Green, A. I.; Morozov, G. I.; Burslem, G. M.; Procko, E.; Sgourakis, N. G. TAPBPR Employs a Ligand-Independent Docking Mechanism to Chaperone MR1 Molecules. *Nat. Chem. Biol.* **2022**, *18*, 859–868.

(24) Eckle, S. B. G.; Birkinshaw, R. W.; Kostenko, L.; Corbett, A. J.; McWilliam, H. E. G.; Reantragoon, R.; Chen, Z.; Gherardin, N. A.; Beddoe, T.; Liu, L.; Patel, O.; Meehan, B.; Fairlie, D. P.; Villadangos, J. A.; Godfrey, D. I.; Kjer-Nielsen, L.; McCluskey, J.; Rossjohn, J. A Molecular Basis Underpinning the T Cell Receptor Heterogeneity of Mucosal-Associated Invariant T Cells. *J. Exp. Med.* **2014**, *211*, 1585–1600.

(25) Boursier, M. E.; Levin, S.; Zimmerman, K.; Kirkland, T. A.; Wood, K. V.; Ohana, R. F. The Luminescent HiBiT Peptide Enables Selective Quantitation of G Protein-Coupled Receptor Ligand Engagement and Internalization in Living Cells. *J. Biol. Chem.* **2020**, *295*, 5124–5135.

(26) McWilliam, H. E. G.; Villadangos, J. A. How MR1 Presents a Pathogen Metabolic Signature to Mucosal-Associated Invariant T (MAIT) Cells. *Trends Immunol.* **2017**, *38*, 679.

(27) Awad, W.; Ler, G. J. M.; Xu, W.; Keller, A. N.; Mak, J. Y. W.; Lim, X. Y.; Liu, L.; Eckle, S. B. G.; Le Nours, J.; McCluskey, J.; Corbett, A. J.; Fairlie, D. P.; Rossjohn, J. The Molecular Basis Underpinning the Potency and Specificity of MAIT Cell Antigens. *Nat. Immunol.* **2020**, *21*, 400–411.

(28) Matsuoka, T.; Motozono, C.; Hattori, A.; Kakeya, H.; Yamasaki, S.; Oishi, S.; Ohno, H.; Inuki, S. The Effects of 5-OP-RU Stereochemistry on Its Stability and MAIT–MR1 Axis. *ChemBioChem* **2021**, *22*, 672–678.

(29) Jeong, Y.-J.; Jung, M. G.; Son, Y.; Jang, J. -H.; Lee, Y.-J.; Kim, S.-H.; Ko, Y.-G.; Lee, Y.-S.; Lee, H.-J. Coniferyl Aldehyde Attenuates Radiation Enteropathy by Inhibiting Cell Death and Promoting Endothelial Cell Function. *PLoS One* **2015**, *10*, e0128552.

(30) Wang, D.; Zhang, L.; Huang, X.; Wang, X.; Yang, R.; Mao, J.; Wang, X.; Wang, X.; Zhang, Q.; Li, P. Identification of Nutritional Components in Black Sesame Determined by Widely Targeted Metabolomics and Traditional Chinese Medicines. *Molecules* **2018**, *23*, 1180.

(31) Wang, Y.; Gao, Y.; Li, X.; Sun, X.; Wang, Z.; Wang, H.; Nie, R.; Yu, W.; Zhou, Y. Coniferyl Aldehyde Inhibits the Inflammatory Effects of Leptomeningeal Cells by Suppressing the JAK2 Signaling. *BioMed. Res. Int.* **2020**, *2020*, 4616308.

(32) Liaqat, H. *Andrographis paniculata*: A Review of its Anti-Cancer Potential. *Medicinal & Aromatic Plants* **2021**,

10, 1–9.

(33) Woo, W. S.; Kang, S. S. A New Phenolic Aldehyde from the Seeds of *Phytolacca americana. Kor. J. Pharmacog.* **1979**, *10*, 83–84.

(34) Luo, D.; Sharma, H.; Yedlapudi, D.; Antonio, T.; Reith, M. E. A.; Dutta, A. K. Novel Multifunctional Dopamine D2/D3 Receptors Agonists with Potential Neuroprotection and Anti-alpha Synuclein Protein Aggregation Properties. *Bioorg. Med. Chem.* **2016**, *24*, 5088–5102.

(35) Zhang, X.-L.; Pan, G.-F.; Zhu, X.-Q.; Guo, R.-L.; Gao, Y.-R.; Wang, Y.-Q. Dehydrogenative β-Arylation of Saturated Aldehydes Using Transient Directing Groups. *Org. Lett.* **2019**, *21*, 2731–2735.

(36) Choi, S.-K.; Mun, G.-I.; Choi, E.; Kim, S.-Y.; Kwon, Y.; Na, Y.; Lee, Y.-S. The Conjugated Double Bond of Coniferyl Aldehyde Is Essential for Heat Shock Factor 1 Mediated Cytotoprotection. *J. Nat. Prod.* **2017**, *80*, 2379–2383.

(37) DiBiase, S. A.; Lipisko, B. A.; Haag, A.; Wolak, R. A.; Gokel, G. W. Direct Synthesis of α,β -Unsaturated Nitriles from Acetonitrile and Carbonyl Compounds: Survey, Crown Effects, and Experimental Conditions. *J. Org. Chem.* **1979**, *44*, 4640–4649.

(38) Kapeller, D. C.; Bräse, S. Versatile Solid-Phase Synthesis of Chromenes Resembling Classical Cannabinoids. *ACS Chem. Biol.* **2011**, *13*, 554–561.

(39) Flaherty, D. P.; Kiyota, T.; Dong, Y.; Ikezu, T.; Vennerstrom, J. L. Phenolic Bis-styrylbenzenes as β-Amyloid Binding Ligands and Free Radical Scavengers. *J. Med. Chem.* **2010**, *53*, 7992–7999.

(40) Sasaki, S.; Kitamura, S.; Negoro, N.; Suzuki, M.; Tsujihata, Y.; Suzuki, N.; Santou, T.; Kanzaki, N.; Harada, M.; Tanaka, Y.; Kobayashi, M.; Tada, N.; Funami, M.; Tanaka, T.; Yamamoto, Y.; Fukatsu, K.; Yasuma, T.; Momose, Y. Design, Synthesis, and Biological Activity of Potent and Orally Available G Protein-Coupled Receptor 40 Agonists. *J. Med. Chem.* **2011**, *54*, 1365–1378.

(41) Yang, L. X.; Huang, K. X.; Li, H. B.; Gong, J. X.; Wang, F.; Feng, Y. B.; Tao, Q. F.; Wu, Y. H.; Li, X. K.; Wu, X. M.; Zeng, S.; Spencer, S.; Zhao, Y.; Qu, J. Design, Synthesis, and Examination of Neuron Protective Properties of Alkenylated and Amidated Dehydro-Silybin Derivatives. *J. Med. Chem.* **2009**, *52*, 7732–7752.

(42) Moriarty, R. M.; Grubjesic, S.; Surve, B. C.; Chandersekera, S. N.; Prakash, O.; Naithani, R. Synthesis of Abyssinone II and Related Compounds as Potential Chemopreventive Agents. *Eur. J. Med. Chem.* **2006**, *41*, 263–267.

(43) Ieda, N.; Nakagawa, H.; Horinouchi, T.; Peng, T.; Yang, D.; Tsumoto, H.; Suzuki, T.; Fukuhara, K.; Miyata, N. Peroxynitrite Generation from a NO-Releasing Nitrobenzene Derivative in Response to Photoirradiation. *Chem. Commun.* **2011**, *47*, 6449–6451.

(44) Varró, G.; Hegedűs, L.; Simon, A.; Balogh, A.; Grün, A.; Leveles, I.; Vértessy, B. G.; Kádas, I. The First Enantioselective Total Synthesis of (−)-*trans*-Dihydronarciclasine. *J. Nat. Prod.* **2017**, *80*, 1909–1917.

(45) Newson, H. L.; Wild, D. A.; Yeung, S. Y.; Skelton, B. W.; Flematti, G. R.; Allan, J. E.; Piggott, M. J. Access to 1,2,3,4-Tetraoxygenated Benzenes via a Double Baeyer-Villiger Reaction of Quinizarin Dimethyl Ether: Application to the Synthesis of Bioactive Natural Products from *Antrodia camphorata. J. Org. Chem.* **2016**, *81*, 3127–3135.

(46) Xu, T.-T.; Jiang, T.-S.; Han, X.-L.; Xu, Y.-H.; Qiao, J.-P. Modular Synthesis of (*E*)-Cinnamaldehydes Directly from Allylarenes via a Metal-Free DDQ-Mediated Oxidative Process. *Org. Biomol. Chem.* **2018**, *16*, 5350–

5358.

(47) Ge, P.; Russell, R. A. The Synthesis of Bisanthraquinone Derivatives as DNA Bisintercalating Agents. *Tetrahedron* **1997**, *53*, 17477–17488.

(48) Schmidtchen, F. P. Probing the Design of a Novel Ditopic Anion Receptor. *J. Am. Chem. Soc.* **1986**, *108*, 8249–8255.

(49) Kaliyaperumal, S. A.; Banerjee, S.; Kumar, U. K. S. Palladium Mediated Intramolecular Multiple C-X/C-H Cross Coupling and C-H Activation: Synthesis of Carbazole Alkaloids Calothrixin B and Murrayaquinone A. *Org. Biomol. Chem.* **2014**, *12*, 6105–6113.

(50) Bauman, J. D.; Patel, D.; Baker, S. F.; Vijayan, R. S. K.; Xiang, A.; Parhi, A. K.; Martínez-Sobrido, L.; LaVoie, E. J.; Das, K.; Arnold, E. Crystallographic Fragment Screening and Structure-Based Optimization Yields a New Class of Influenza Endonuclease Inhibitors. *ACS Chem. Biol.* **2013**, *8*, 2501–2508.

(51) Kitamura, T. New Experimental Approaches in Retrovirus-Mediated Expression Screening. *Int. J. Hematol.* **1998**, *67*, 351–359.

(52) Yokosuka, T.; Takase, K.; Suzuki, M.; Nakagawa, Y.; Taki, S.; Takahashi, H.; Fujisawa, T.; Arase, H.; Saito, T. Predominant Role of T Cell Receptor (TCR)-α Chain in Forming Preimmune TCR Repertoire Revealed by Clonal TCR Reconstitution System. *J. Exp. Med.* **2002**, *195*, 991–1001.